AD-A110 459 NAVAL RESEARCH LAB . WASHINGTON DC F/G 20/4
STEADY HYDRODYNAMIC LOADS DUE TO VORTEX SHEDDING FROM THE OTEC --ETC(U)
JAN 82 O M GRIFFIN NOAA-NA-80-AA6-03362
UNCLASSIFIED NRL-MR-4698 NL

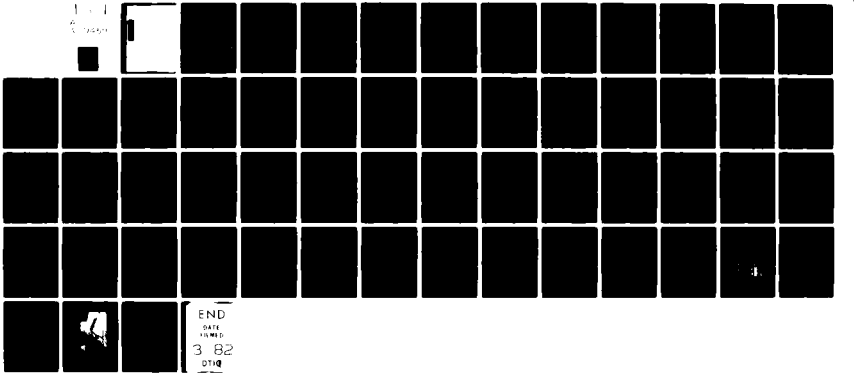

END
DATE FILMED
3 82
DTIC

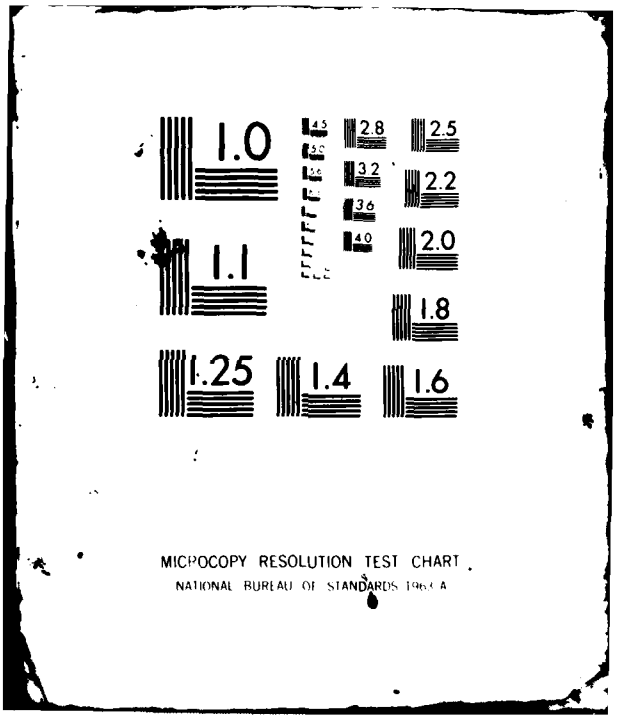
1.0
1.1
1.25
1.4
1.6
1.8
2.0
2.2
2.5
2.8
3.2
3.6
4.0
MICROCOPY RESOLUTION TEST CHART
NATIONAL BUREAU OF STANDARDS 1963 A

(1) NRL-MR-4698

SECURITY CLASSIFICATION OF THIS PAGE (When Data Entered)

REPORT DOCUMENTATION PAGE

READ INSTRUCTIONS BEFORE COMPLETING FORM

1. REPORT NUMBER: NRL Memorandum Report 4698	2. GOVT ACCESSION NO.: AD-A114 459
3. RECIPIENT'S CATALOG NUMBER:	
4. TITLE (and Subtitle): STEADY HYDRODYNAMIC LOADS DUE TO VORTEX SHEDDING FROM THE OTEC COLD WATER PIPE	5. TYPE OF REPORT & PERIOD COVERED: Final
	6. PERFORMING ORG. REPORT NUMBER:
7. AUTHOR(s): Owen M. Griffin	8. CONTRACT OR GRANT NUMBER(s): NOAA Project No. NA 80AAG 03362
9. PERFORMING ORGANIZATION NAME AND ADDRESS: Naval Research Laboratory, Washington, DC 20375	10. PROGRAM ELEMENT, PROJECT, TASK AREA & WORK UNIT NUMBERS: NRL Problem 0275-0
11. CONTROLLING OFFICE NAME AND ADDRESS: Office of Ocean Technology & Engineering Services, NOAA, Rockville, MD 20852	12. REPORT DATE: January 13, 1982
	13. NUMBER OF PAGES: 56
14. MONITORING AGENCY NAME & ADDRESS(if different from Controlling Office)	15. SECURITY CLASS. (of this report): Unclassified
	15a. DECLASSIFICATION/DOWNGRADING SCHEDULE:

16. DISTRIBUTION STATEMENT (of this Report)

Approved for public release; distribution unlimited.

17. DISTRIBUTION STATEMENT (of the abstract entered in Block 20, if different from Report)

18. SUPPLEMENTARY NOTES

DTIC ELECTE FEB 4 1982 S D A

19. KEY WORDS (Continue on reverse side if necessary and identify by block number)

Ocean engineering
Ocean thermal energy conversion
Vortex-excited oscillations
Vortex shedding

20. ABSTRACT (Continue on reverse side if necessary and identify by block number)

This report is limited in scope to consideration of the problems caused by vortex shedding from flexible, bluff cylinders in steady current flows, as these problems apply to the OTEC cold water pipe. In particular, the steady deflections caused by the amplified drag forces that accompany vortex-excited oscillations are considered. Emphasis placed upon the discussion of design methods, applications of these methods to practical problems, and comparison with available experimental data. A discussion is given of laboratory and field studies that have been conducted with model OTEC cold water pipes.

(Continued)

DD FORM 1 JAN 73 1473 EDITION OF 1 NOV 65 IS OBSOLETE
S/N 0102-014-6601

SECURITY CLASSIFICATION OF THIS PAGE (When Data Entered)

20. ABSTRACT (Continued)

Various devices that have been developed for the suppression of vortex-excited oscillations also are discussed. A comparison is made of the effectiveness of various suppression devices and procedures, and practical approaches to implementing their application are presented. The implications of vortex-induced hydrodynamic drag and the suppression of vortex-excited oscillations in OTEC cold water pipe design are discussed briefly.

CONTENTS

FOREWORD AND ACKNOWLEDGMENTS

This report has been prepared by the Naval Research Laboratory as part of the OTEC cold water pipe technology development program at the Office of Ocean Technology and Engineering Services, National Oceanic and Atmospheric Administration. The cooperation and helpful comments and criticisms of Dr. R. Scotti, formerly of OTES, NOAA and Mr. L. Fischer of OTES, NOAA during the preparation of this report are appreciated. The author also wishes to thank Dr. R. King and Mr. M. J. Every of BHRA Fluid Engineering for providing detailed reports of recent BHRA experiments.

MAGNITUDE OF THE PROBLEM

Problems that are caused by vortex shedding and the vortex-excited oscillations of marine structures often have been ignored in the past, largely because reliable experimental data and design methods have not been available. However, as marine construction has moved into deeper water and into harsher operating environments such as the North Sea, the need to design slender, flexible structures and structural members against vortex shedding-related problems has increased in importance. The steady and unsteady vortex-excited hydrodynamic forces and their associated deflections and vibrations cause amplified stress levels and fatigue, and they often lead to structural damage and eventually to failure.

Many types of marine structures are susceptible to vortex-excited oscillations. These include the risers and conductor tubes that are employed in offshore oil exploration and production, deep water pipelines, and members of jacketed structures. Deep water piling installation and driving operations also are hampered at times by problems arising from vortex shedding. Several case studies have been documented in the literature in recent years. Among these was the installation of an offshore oil terminal at Immingham in the United Kingdom during late 1969. Significant vortex-excited motions were encountered during the installation of pilings in a tidal flow, and these oscillations caused severe construction difficulties. A wide ranging test program was conducted both at the field sites and in various laboratories in order to determine the causes of the vibrations and to devise means of preventing them.

Laboratory tests and design studies were conducted in the mid 1970's to develop a riser fairing that would allow a semisubmersible drilling vessel to operate off the coast of Brazil in 152 m (500 ft) of water and in strong surface currents up to 4.1 m/s (8 kt). These tests resulted in the development of an economical and practical fairing device to suppress any vortex-excited oscillations.

The recent underwater installation of 187 m (610 ft) long foundation piles for the Shell Oil production platform in the Cognac field of the Gulf of Mexico presented several potential problems due to vortex-excited oscillations. Currents of sufficient magnitude to cause resonant oscillations of the piles had been measured at the installation site which has a water depth of 350 m (1150 ft). The anticipated problems included the "stabbing" of oscillating piles into sleeves in the platform base section, and oscillations of the stabbed piles during the subsequent driving operation. Laboratory tests were conducted to determine the vulnerability of model piles to resonant vortex excitation and suppression devices were developed. Estimates of static and dynamic stress levels during Cognac pile driving operations showed that cross flow vortex-excited oscillations would triple the maximum stresses relative to the nonvibrating pile. Under certain circumstances a fatigue life of four days was predicted for the bare piles when their exposed length of 130 m (425 ft) was resonantly excited by currents with magnitudes of 0.46 m/s (0.9 kt).

The water depth of 18 m (59 ft) at Immingham was relatively shallow, and since then marine construction has moved into deeper water and more harsh operating regimes such as the North Sea. In 1979 the jack-up rig "Offshore Mercury" was drilling for the British Gas Corporation in 61 m (200 ft) of water in the English Channel near the Isle of Wight. Problems were encountered with vibrations of a drill pipe due to vortex shedding. The rig was operating in a 1.5 m/s (3 kt) current and the pipe, 610 mm (2 ft) in diameter, was oscillating with a displacement amplitude of ± 0.5 diameters perpendicular to the current direction. The Reynolds number of the vortex wake was about 10^5. Not only was the drill pipe resonantly oscillating, but also drilling machinery on the deck of the rig was oscillating in unison with it. These resonant vibrations caused two fatigue failures of the drill pipe. Prior to the time when an acceptable solution was devised, approximately $5 million in losses were incurred.

The cold water pipe of an OTEC plant will be a long slender marine structure of cylindrical cross-section that typically will extend to depths of 1000 m (3280 ft) in the ocean from the platform of the

plant. It is precisely this type of marine structure that is most susceptible to resonant excitation by vortex shedding due to the relative motion between the pipe and the water. The cold water pipe is considered by some to be the greatest engineering problem facing OTEC, and the reliable design of the pipe to withstand environmental forces over a long (30 year) life time is a principal objective of the on-going OTEC development program. Reliable procedures to design marine structures against vortex shedding-related problems have been proposed, but none of these have been applied directly to the design of the cold water pipe. It is only through laboratory and at-sea tests similar to those summarized above and described in detail later in this report that reliable procedures for the design of the OTEC cold water pipe can be developed, verified, and put into engineering practice.

STEADY HYDRODYNAMIC LOADS DUE TO VORTEX SHEDDING FROM THE OTEC COLD WATER PIPE

1. INTRODUCTION AND BACKGROUND.

1.1 Objectives and Justification.

It is often found that unstreamlined or bluff structures display oscillatory instabilities when exposed to wind or current flow past them. One common mechanism for generating these resonant, flow-excited oscillations is the organized and periodic shedding of vortices as the flow separates alternately from opposite sides of the body. The flow field exhibits a dominant periodicity and the body is acted upon by time-dependent pressure loads which result in steady and unsteady drag forces in line with the flow as well as unsteady lift or side forces in the cross flow direction. If the structure is flexible and lightly damped, then resonant oscillations can be excited normal or parallel to the incident flow direction. For the more common cross flow oscillations, the body and wake oscillate in unison near one of the natural frequencies of the structure, and near the Strouhal frequency at which pairs of vortices would be shed if the structure were stationary. This phenomenon is commonly termed "lock-on" or "wake capture."

Vortex-excited oscillations of marine structures and cables result in reduced life due to fatigue, amplified hydrodynamic forces, and often lead to structural damage and to destructive failures. Flow-excited oscillations very often are a critical factor in the design of risers and offshore platforms, since these complex structures usually have bluff cylindrical elements which are prone to vortex shedding in an incident current. The cold water pipe of an ocean thermal energy conversion (OTEC) plant is typically a bluff, flexible cylinder with a large aspect ratio (L/D = length/diameter), and it is likely to be susceptible to current-induced vortex excitation. Thus an understanding of the nature of the

Manuscript submitted October 27, 1981.

fluid/structure interaction and the resultant flow-induced hydrodynamic loads is an important consideration in the reliable design of the OTEC cold water pipe and its associated mooring and riser cable systems. The cold water pipe is often cited as the greatest engineering problem in OTEC development.

Several recent texts, design manuals, and survey articles and reports have considered in various contexts the problems associated with vortex-excited oscillations. These include design manuals on the dynamics of marine structures [1], books on the general field of flow-induced vibrations [2], and articles on vortex shedding problems relative to marine structures [3]. Also, a lengthy but selective review article on the general topic of vortex-induced oscillations [4] is included. The most recent critical survey and design report is directly related to the OTEC cold water pipe technology development program [5].

1.2 Scope of the Investigation.

This report is limited in scope to consideration of the problems caused by vortex shedding from flexible, bluff cylinders in steady current flows. *In particular*, the steady deflections caused by the amplified drag forces that accompany vortex-excited oscillations are considered. Emphasis is placed upon the development of design procedures, application of these procedures in practice, and comparisons with laboratory-scale data. A comparison is made with the limited laboratory and field studies that have been conducted with model OTEC cold water pipes.

Also discussed are various means that have been developed for the suppression of vortex-excited oscillations. A comparison is made of the effectiveness of various suppression devices and procedures, and practical approaches to implementing their application are presented. The implications of vortex-induced hydrodynamic drag and vortex suppression in OTEC cold water pipe design are then discussed.

There are complex and important problems associated with the shedding of vortices from cylinders in waves, and from the combined action of waves and currents. However, these even more complex fluid/structure interactions are not considered in this report. These problems are considered

to some extent in a recently published working guide for estimating the hydrodynamic loadings on marine structures [6].

1.3 Background.

As an essential part of its operation, an OTEC power plant withdraws large amounts of cold water from the deeper layers of the ocean through a long cold water pipe (CWP) suspended from the OTEC platform. For a plant generating 40 MW_e of electrical power, the CWP can be as large as 9.2 m (30 ft) in diameter and 1000 m (3,280 ft) long. When deployed in the ocean environment the CWP will experience hydrodynamic forces, both directly due to currents and waves as well as indirectly through forces transmitted by the motions of the platform. An understanding of and a means of designing for these forces are essential steps toward ensuring the successful operation of OTEC plants.

An ocean engineering technology development program has been initiated for the Department of Energy by the National Oceanic and Atmospheric Administration (NOAA), Office of Ocean Technology and Engineering Services (OTES). The purpose of this program is to develop reliable engineering design methodologies for the prediction of the hydroelastic response of the CWP, the coupled platform/CWP, and the platform station-keeping and seawater systems throughout their life cycles. The 9.2 m (30 ft) diameter, 1000 m (3,280 ft) long CWP prototype presently envisioned for a 40 MW_e plant will operate at cold water flow rates up to 3.44×10^4 gallons per second (13×10^4 liters per second). It is to have an expected life of 30 years.

The critical aspects of the NOAA/DOE cold water pipe technology development plan fall into the following three categories:

- Characterization of engineering properties of candidate CWP materials, especially with regard to strength and long term cyclic fatigue;
- Determination of the response of a CWP during tow-to-site and deployment operations;

- Determination of the response of the platform/CWP system to all environmental loads during both normal operations and storm survival.

An overview of the CWP design and development program is presented in a recent paper [7]. Many of the cold water pipe and ocean engineering problems facing OTEC are discussed in several related papers published as a single volume [8].

Preliminary design concepts for the CWP that have been studied [9] comprise the following general categories:

- Rigid-wall pipe with or without articulated joints;
- Compliant pipe;
- Bottom-mounted pipe.

Figures 1, 2, and 3 show some typical OTEC cold water pipe configurations. Materials under consideration for CWP construction include steel, concrete, fiber reinforced plastic (FRP), thermoplastics and elastomers/fabrics.

2. RECENT MEASUREMENTS OF STEADY HYDRODYNAMIC DRAG FORCES.

A significant effect that accompanies the resonant cross flow oscillations of structures and cables due to vortex shedding is an amplification of the steady drag force (or drag coefficient). The drag amplification under a variety of conditions has been measured and the results have been reported by Griffin and Ramberg [10]. A procedure for applying these measurements to marine cable structures was developed by Skop, Griffin and Ramberg [11]. This procedure has been generalized to the case of flexible, cylindrical marine structures by Griffin [5] in a study of the OTEC cold water pipe's susceptibility to flow-induced oscillations. The step-by-step approach is outlined in Figure 4.

Measurements of the vortex-excited cross flow oscillations of model marine piles were made by Fischer, Jones and King [12, 13] as part of a study of pile installation during construction of the Cognac platform in the Gulf of Mexico. The steady deflection at the free end of the model pile also was measured; the model was a simple, uniform cantilever beam with no tip masses, fully immersed in water, and normal to the incident flow. The relative density of the flexible cylinder was varied in order to conduct the experiments under different conditions. For low flow velocities the measured and predicted tip deflections coincided when the pile was effectively stationary as shown in Figure 5. The deflection was predicted by assuming a uniform loading

$$w(x) = 1/2\,\rho\ V^2 D\ C_D(x)$$

over the length of the flexible beam in which the (constant) drag coefficient $C_D = 1.2$.

When the critical flow velocity for the onset of the vortex-excited oscillations was exceeded, the measured steady deflections in line with the flow departed significantly from the predicted reference curve. The results are plotted in Figure 5. For the lower values of relative density the flow velocities above the threshold velocity caused steady deflections of up to twice the value predicted by assuming $C_D = 1.2$. For the higher values of relative density, the steady deflections of the model diverged from the predicted curve, reached a maximum, and then returned to the predicted curve as the flow velocity was increased still further. The region of divergence corresponds directly to the range of resonant,

large amplitude cross flow oscillations that also were measured by Fischer, Jones, and King [12, 13]. For example, the tip of the SG = 3.5 pile experienced a steady deflection in line about 1.3 diameters at a water velocity of 13 in/sec (1.08 ft/sec). At this same flow velocity the unsteady cross flow displacement amplitude was ±1.4 to 1.5 diameters. If the pile was restrained from oscillating, then the steady deflection of the tip was predicted to be 0.6 diameters at the same flow velocity.

A program of tests, conducted at the David Taylor Naval Ship R&D Center during the 1940's and declassified in the past few years, resulted in a strong resonance due to vortex shedding when a bare circular cylinder was towed through water and underwent large-amplitude cross flow oscillations [14]. This cylinder later was fitted with various vortex suppression devices in order to investigate their efficiency in suppressing the cross flow oscillations that the bare cylinder underwent. The drag on the cylinder was measured over a range of towing speeds up to 10 kts and the results are plotted in Fig. 6. A clear resonance occurred near V = 4 kts and the drag force (and coefficient C_D) was increased by a factor of 220 percent at a towing speed of 4.25 kts. At this and nearby towing speeds, the cross flow displacement amplitude of the cylinder was ±1.5 to 2 diameters [14]. When the cylinder was towed at speeds above and below the resonance, the usual

$$\text{Drag} \propto (\text{Flow Speed})^2$$

dependence was obtained.

3. CALCULATION OF THE STEADY IN LINE DEFLECTIONS OF MARINE STRUCTURES

3.1 Calculation of Drag-Induced Deflections

It is possible to predict the steady deflection of the oscillating cylinder in Fig. 5 by treating it as a long, flexible beam since the cylinder had a length/diameter ratio of $L/D = 52$. The equation for the steady deflection $Z_s(x)$ of a simple, flexible cantilever can be written as

$$Z_s'''' = K\ C_D(x), \tag{1}$$

where

$$K = \frac{3}{2}\frac{\rho}{g_c}\frac{V^2 L}{G}. \tag{2}$$

The primes denote the derivative taken with respect to x. Here $g_c = 32.2\ \text{lb}_m\ \text{ft/lb}_f\ \text{sec}^2$ and the stiffness $G = 3EI/L^3$. The steady deflection Z_s is measured in multiples of the diameter D and the displacement x (measured from the clamped end $x = 0$) is measured as a fraction of the length L. Tensile forces are neglected for this simple example, although in the case of more complex structures such as risers, conductor pipes, and real OTEC cold water pipes the tension variations in the axial direction cannot be neglected in either static or dynamic analyses [15].

The distributed loading on the right hand side of Eq. (1) is due to the drag forces which vary locally with the vortex-excited displacement amplitude along the cylinder. The drag coefficient C_D (normalized by the stationary cylinder value C_{D0}) is plotted in Fig. 7 as a function of the response parameter

$$w_r = (1 + 2\bar{Y}/D)\ (\text{St}\ V_r)^{-1}. \tag{3}$$

Both the reduced velocity $V_r = V/f_n D$ and the local displacement amplitude $\bar{Y}/D$ are accounted for in the expression for w_r. St is the Strouhal number for $\bar{Y}/D = 0$. For the purposes of this example the complete least-squares fit to the data given in Fig. 7 is approximated by

$$C_D/C_{D0} = A_1 + B_1 w_r. \qquad \begin{matrix} A_1 = 0.54 \\ B_1 = 0.88 \end{matrix} \tag{4}$$

This is a reasonable approximation for the present case. Equation (4), which in effect yields the dependence of the drag coefficient C_D on vortex-excited displacement amplitude $\bar{Y}$ and flow velocity V, can be expanded to

$$C_D = C_{D0}\{A_1 + B_1(1 + 2\bar{Y}(x)/D)\ (St\ V_r)^{-1}\}$$

The fundamental normal model of vibration of a cantilever beam is accurately approximated by (Bishop and Johnson, Ref. 16)

$$y = \bar{Y}_{MAX}\left[1 - \cos\left[\frac{\pi}{2}x\right]\right], \tag{5}$$

where the tip displacement is given by $\bar{Y}_{MAX}$. Equation (4) then is of the form

$$C_D = C_{D0}\left\{A_1 + B_1A_2\left[1 + B_2\left[1 - \cos\left[\frac{\pi}{2}x\right]\right]\right]\right\} \tag{4a}$$

where

$$A_2 = (St\ V_r)^{-1}$$
$$B_2 = 2\ \bar{Y}_{MAX}/D.$$

The beam equation then becomes

$$Z_s'''' = K_1 - K_2 \cos\left[\frac{\pi}{2}x\right] \tag{6a}$$

where

$$K_1 = K\ C_{D0}\ [A_1 + B_1\ A_2\ (1 + B_2)] \tag{6b}$$

and

$$K_2 = K\ C_{D0}\ B_1\ A_2\ B_2. \tag{6c}$$

The appropriate boundary conditions for a cantilever beam are

$$Z_s(0) = Z_s'(0) = 0$$
$$Z_s''(1) = Z_s'''(1) = 0.$$

It is assumed as a first approximation that any differences between the normal mode shape and the forced mode shape are negligible. King [13] has found that within reasonable limits cylinders oscillating due to vortex shedding do so normal modes. The ramifications of this finding are discussed by Every, King and Griffin [17].

When Eq. (6a) is integrated four successive times and the boundary conditions are applied, the solution is

$$Z_s(x) = K_1\frac{x^4}{24} + K_2\left(\frac{2}{\pi}\right)^4\left[1 - \cos\left(\frac{\pi}{2}x\right)\right] - \left[K_1 - K_2\left(\frac{2}{\pi}\right)\right]\frac{x^3}{6} + \left[\frac{K_1}{2} - K_2\left(\frac{2}{\pi}\right)\right]\frac{x^2}{2}. \tag{7}$$

The steady deflection at the tip in the fundamental mode is given when Eq. (7) is evaluated at $x = 1$, or

$$Z_s = \frac{1}{8}K_1 - K_2\left[\frac{2}{3\pi} - \left(\frac{2}{\pi}\right)^4\right]. \tag{7a}$$

In terms of the various coefficients in Eq. (4), this latter equation is

$$Z_s = K\,C_{D0}\{0.125[A_1 + B_1A_2\,(1 + B_2)] - 0.048\,B_1A_2B_2\}. \tag{8}$$

The static bending moment on the cylindrical beam can be calculated from the equation

$$\overline{M} = EI\,\overline{Z}_s''. \tag{9a}$$

This equation can be written in nondimensional form as

$$M = \frac{\overline{M}L^2}{EID} = Z_s''. \tag{9b}$$

From the previous solution,

$$Z_s'' = K_1\frac{x^2}{2} + K_2\left(\frac{2}{\pi}\right)^2\cos\left(\frac{\pi}{2}x\right) - \left[K_1 - K_2\left(\frac{2}{\pi}\right)\right]x + \left[\frac{K_1}{2} - K_2\left(\frac{2}{\pi}\right)\right]. \tag{10a}$$

and at $x = 0$, this equation reduces to

$$Z_{s,x=0}'' = \frac{K_1}{2} - \left(\frac{2}{\pi}\right)\left(1 - \frac{2}{\pi}\right)K_2.$$

The bending moment at the base of the beam, $x = 0$, is then

$$M = \frac{\overline{M}L^2}{EID} = \frac{1}{2}\left[K_1 - 2\left(\frac{2}{\pi}\right)\left(1 - \frac{2}{\pi}\right)K_2\right]$$

where K_1 and K_2 again are defined by Eqs. (6b) and (6c). Then the equation for the bending moment is

$$M = \frac{\bar{M}L^2}{EID} = \frac{1}{2}KC_{D0}\left[A_1 + B_1A_2(1 + B_2) - 2B_1A_2B_2\left\{\frac{2}{\pi}\right\}\left\{1 - \frac{2}{\pi}\right\}\right]. \tag{11}$$

The coefficients K, C_{D0}, A_1, A_2, B_1, and B_2 all have been defined previously in this section. For a stationary cylinder $K_1 = KC_{D0}$ and $K_2 = 0$, so that

$$M_0 = \frac{1}{2}\,KC_{D0}. \tag{12}$$

The amplification of the base bending moment then is

$$\frac{M}{M_0} = \left[A_1 + B_1A_2(1 + B_2) - 2B_1A_2B_2\left\{\frac{2}{\pi}\right\}\left\{1 - \frac{2}{\pi}\right\}\right]. \tag{13}$$

This is the ratio of the bending moment M on the cylinder oscillating due to vortex shedding, and the bending moment M_0 that is induced when the cylinder is restrained from oscillating.

3.2 Comparison with Experiments

Equation (8) can be used to predict the steady deflection of the model pile and to compare the predicted deflection with King's measurements. The model was a flexible circular cylinder with the properties given in Table 1. The specific gravity or relative density of the basic model pile was changed by filling it with various substances (lead shot, water, sand, etc.). Three cases are predicted in Table 2 and excellent agreement is achieved with the measured data from Fig. 5. The average drag amplification was determined by integrating Eq. (4a) over the length of the beam. At the peak vortex-excited displacement amplitude of $\bar{Y}/D = \pm 1.2$ to 1.4, the average drag coefficient over the length of the cylinder increased by a factor of 1.6 to 1.9. These amplification factors result in estimated drag coefficients of $C_D = 2.0$ to 2.3 as a result of the oscillations.

This increased drag causes the steady deflection at the tip of the cantilever to increase by a factor of up to two from the values predicted when the cylinder is restrained from oscillating. The results in Table 2 also show that the predicted bending moments at the base of the vibrating cantilever beam are amplified by factors of $M/M_0 = 1.9$ to 2.5 from the corresponding condition if the beam was stationary.

Some examples of the agreement between the predicted and measured steady deflections are shown in Fig. 8. The predictions and measurements are in reasonable agreement, considering that Eq. (7) is based upon limited experimental data from a variety of sources. Further examples of this agreement for the remaining cases in Fig. 5 are given by Every, King and Griffin [17].

The drag on the cylinder used by Grimminger [14] resulted in a drag coefficient of $C_D = 2.2$ when the cylinder was oscillating at the peak cross flow displacement amplitudes of $Y/D = \pm 1.5$ to 2. When the cylinder was restrained from oscillating, the drag coefficient was $C_{D0} = 1$.

It can be seen throughout the lock-on range that the effective drag coefficient increases as a function of cross flow amplitude. In some cases the effective drag coefficient is up to 250% larger than the stationary cylinder drag coefficient. This results in high steady stresses when the oscillatory stresses also are at their highest. The cumulative effects of these stresses must be investigated in any design assessment.

The steady deflection calculations that are discussed in this section represent only the simplest of example problems. However, the drag amplification equation given in Fig. 7 readily can be employed together with a more complex steady deflection equation than the simple cantilever discussed here. In the case of a real cold water pipe with a bottom weight, internal water flow, and tension members or a marine riser with variable tension, pressure differences, and buoyancy elements the drag amplification effect can be introduced into the more complex numerical simulation that is required. Also, the reliability of applying the concept of hydrodynamic drag amplification as described here to prototype and full-scale structures will be increased when more extensive experimental results such as those Fig. 7 are available over the applicable range of Reynolds numbers.

4. OTEC COLD WATER PIPE APPLICATIONS

There are relatively few studies of vortex shedding effects on the OTEC cold water pipe. One related NRL report [5] discusses the design aspects of problems caused by vortex-excited oscillations due to steady current flow past the pipe. In another study experiments were conducted to investigate the effects of shear (nonuniform flow) on cylinders at large Reynolds numbers; this work was oriented specifically to OTEC cold water pipe applications [18]. Some preliminary field experiments were conducted with a PVC pipe, 0.22 m (8.6 in) in diameter and 21.4 m (70 ft) long, under both grazing (slow, steady motion) and moored conditions [19]. The upper end of the 1/30-scale model pipe was attached to a test platform by a universal joint, and the lower end was connected to a 454 kg (1000 lb) weight.

A preliminary series of laboratory experiments also was conducted with a flexible, stainless steel cylinder to model the cold water pipe [20]; however, only limited results were obtained from these experiments. In another series of towing channel experiments, a compliant wall OTEC cold water pipe model underwent extensive testing [21]. The cylinder, nominally 0.24 m (9.25 in) in diameter and 2.8 m (9.25 ft) long, experienced large amplitude cross flow oscillations in water over a wide range of conditions.

4.1 Field Experiments

The measured pipe response during one of the TRW grazing test runs is shown in Figure 9. The average towing speed was 0.74 m/s (2.44 ft/sec) and the resonance was clearly in the third (n=3) mode [19]. The pipe was fitted with five strain gages along its length to measure the stresses induced by any resonant oscillations that occurred. The individual stress curves in Fig. 9 were measured at five time intervals of $\Delta t = 1.0$ sec. Plots of power spectral density clearly show a resonance at $f = 0.88$ Hz with a small contribution at $2f$. The results obtained from the TRW ocean tests are summarized in Table 3. For the case just discussed, in the $n = 3$ mode the reduced velocity based upon f, the tow speed V, and the pipe diameter D is $V_r = 3.86$, which suggests that the oscillations occurred at the low velocity end of the third mode resonance. A second test run also is listed in Table 3. The resonance in

that case clearly is in the second mode, $n = 2$, as shown in Fig. 10 and by the related power spectral density results for that test run in Ref. 19. This second resonant response appears to occur toward the high velocity end of the second mode resonance, at $V_r = 6.3$.

The response of the pipe in two different modes at nearly identical towing speeds is not unusual. A similar case is shown in Fig. 10 where the resonant cross flow response of a towed marine cable is plotted [22, 23]. The cable underwent locked-on strumming oscillations as shown by the displacement amplitude and vibration (shedding) frequency data shown in Fig. 10 and by a spectral analysis of the data (not shown). There is some overlap in the response between the $n = 1$ and $n = 2$ modes of the cable, and it is likely that the two cold water pipe test runs exhibit similar response behavior. This anomaly can be triggered by small changes in the test parameters such as towing speed, tension, etc. The TRW model pipe was tuned to respond at a towing speed of 1 kt (1.69 ft/sec), and it is likely that the pipe resonance at that towing speed, probably in the $n = 2$ mode, would be amplified still further from the stress levels shown in Fig. 9.

4.2 Towing Channel and Small-Scale Laboratory Experiments

A compliant wall cold water pipe model underwent extensive towing tests in a water channel [21]. The pipe was constructed of urethane-coated nylon fabric which formed the pressurized, annular compliant pipe body. The upper end of the pipe section was attached to the towing carriage and the lower end to a ballast weight. The pipe natural frequencies were measured as a function of pipe annulus and core pressures; and cross flow displacement amplitudes, frequencies and towing speeds were measured for a variety of pipe annulus pressurization conditions.

The model experiments were conducted at Reynolds numbers near $Re = 2 \times 10^5$ and a typical example of the results is given in Figure 12. The annulus and core pressures of the pipe, PA and PC respectively, are given in the figure; the values shown correspond to a natural frequency (in water) of $f_n = 0.075$ Hz. The peak displacement amplitude of the model is $\bar{Y}/D = \pm 1.25$ from equilibrium, and this is typical of light cylinders in water [5]. The reduced velocity at the peak displacement is

$V_r = V/f_n D = 6.2$; again this is typical of cylinders oscillating in water. The overall range of reduced velocities over which $\bar{Y} > \pm 0.5D$ is $V_r = 5.5$ to 13, which as before is more or less typical of experiments conducted in water. The broad range of V_r above the peak displacement amplitude is probably due to the almost neutral buoyancy of the inflatable pipe. An upper limit of $V_r = 10$ to 11 more often is observed for cylinders which are not neutrally buoyant or nearly so.

The cylinder vibrated in a pendulum-like mode and the steady tip deflection was measured over the complete range of towing speeds. The steady tip deflection at the peak displacement amplitude shown in Fig. 12 was about $\bar{Z}_s = 1.2$ to $1.4D$. A similar tip displacement was obtained for another test run when the ballast weight was increased to 38 kg (83 lb) and the unsteady displacement amplitude was $\bar{Y} = \pm 1.2D$. As compared to the resonance shown in the steady tip displacements at the higher values of relative density (SG = 2.5 and 3.5) in Fig. 5, the tip displacements at low values of SG increase monotonically with towing speed. However, the usual

$$\text{Drag } \alpha \text{ (Current Speed)}^2$$

law is not followed as in the region outside of the resonance in Figs. 5 and 6, but instead the drag on nearly neutral bouyant pipe increases with flow speed at a power greater than $n = 2$. Similar results were obtained by King [13] for the SG = 1.5 and 2.0 experiments in Fig. 5. This effect apparently is due to the near-neutral buoyancy of the relevant cylinders in both experiments, though a complete explanation is lacking at this time. Estimates of the average drag coefficient required to produce these steady tip deflections at resonance were as high as $C_D = 2.2$ [21].

A hydroelastic experiment with a small model OTEC pipe was reported in 1979 [20]. The water-filled steel tube model was very small, 5.3 mm (0.21 in.) in diameter and 457 mm (18 in.) long with a 0.127 mm (0.005 in.) wall thickness, but it was "tuned" to oscillate resonantly due to vortex shedding. A peak cross flow displacement amplitude of $\bar{Y} = \pm 1.7D$ was measured in the cylinder's first cantilever mode at $V_r = 5.8$ (based upon the natural frequency, $f_n = 11.8$ Hz, of the cylinder). Appreciable in-line oscillations also were measured [20].

These are the only experimental findings that relate specifically to the OTEC cold water pipe. However, there is a considerable experimental data base relating to the vortex-excited oscillation of circular cylindrical members in general. These data are reviewed and discussed in Refs. 5 and 22. The steps required to assess the susceptibility of a structure to vortex-excited oscillations are summarized in the Appendix of this report.

5. SUPPRESSION OF VORTEX-EXCITED OSCILLATIONS

Vortex-excited oscillations often can be reduced in level or suppressed by the installation of external devices that modify the flow field about the structure. Helical fins, porous shrouds and streamlined fairings have been used with some success [24, 25, 26, 27], but in general it is preferable to design the structure itself to avoid the vortex-excited oscillations whenever possible. Every and King [26] discuss a recent experimental study of various vortex suppression devices. These experiments were conducted to find an acceptable solution to problems caused by vibrating drill pipes that were attached to a jack-up rig in the North Sea. Zdravkovich [28], in a recent study, has catalogued and classified virtually every known vortex suppression device. In that study the effectiveness of the various devices is discussed and rated, drag coefficients are listed, and recommendations of optimum configurations are made. The study of Zdravkovich is especially valuable because he discusses in detail not only effective devices for vortex suppression and their mechanisms (when known), but also he gives considerable attention to devices that did not suppress the vortex-excited oscillations (sometimes the latter were actually increased!) and to why the devices failed.

The difficulty in developing an effective means of oscillation suppression lies in the dependence of a device's effectiveness on several factors. These include the Reynolds number of the flow, the structural damping of the cylinder, and the geometry of the device. Another factor is the vortex-excited displacement amplitude itself, and consequently the reduced damping. The large cross flow diplacement amplitudes that are common to marine structures (see Figs. 14 and 17) give ample evidence of the difficulties involved in devising an optimally effective means of vortex shedding suppression for offshore applications.

5.1 Means for Suppressing Vortex-Excited Oscillations.

There are essentially three primary methods of preventing the in line and cross flow oscillations, as described in detail by Hallam, Heaf and Wootton [1], Dean and Wootton [29], and King, Prosser and Verley [25]. These are:

(a) Control of the structural design so as not to exceed the critical values of reduced velocity, $V_r = V/f_n D$;

(b) Structural design for sufficiently large mass and damping;

(c) Modification of the flow field around the cylinder altering the flow and/or the structural shape.

The first two methods were described in detail in a previous report [5]. The remainder of this section will focus on the use of various types of spoilers to reduce the oscillations, since the implementation of the first two methods may be difficult because of operational requirements in a marine environment.

There are generally three types of devices which have been employed with success to reduce vortex-excited oscillations of flexible structures (except for cables, which will be discussed briefly later). These are strakes, or helically-wound fins, porous shrouds which fit over the cylindrical structure, and nearwake stabilizers (fairings) and fins in various configurations. Some typical examples given by Every, King and Griffin [17] are shown in Fig. 13.

Strakes. Helical strakes have been widely employed in reducing the wind-excited oscillations of large chimneys. Strakes, however, cause difficulties in installation and handling and tend to increase the steady drag coefficient. A straked cylinder has a drag coefficient of $C_d \cong 1.4$ [28]. Hallam, Heaf and Wootton [1] discuss the optimum strake configuration; this is three helically-wound fins about 10 percent of the cylinder diameter, with a pitch of 5. Semirigid strake windings have been developed specifically for offshore applications [27,30]; an increase of 10 percent or more over the steady drag on the bare cylinder is estimated.

Shrouds. Perforated shrouds have been employed successfully to eliminate the cross flow and in line motions due to vortex shedding [25,26,30]. The shroud is effective for all approach flow directions. An optimum shroud geometry should have a diameter 20 percent greater than the cylinder and an open area ratio of 36 percent, and should extend over 20 percent of the wetted length of the cylinder [25]. Information that is available suggests that marine growth does not reduce the shroud's effectiveness.

In a variation of the shroud, Wong [32] has proposed the use of an array of longitudinal slats attached to the cylindrical members. The slats are evenly spaced around the circumference of the cylinder and are held away from it by some means. Laboratory experiments have shown that this device is effective in reducing the oscillations to tolerable levels. According to Wong, the spacing between the slats and cylinder, the slat width, and open area ratio should be optimized for each individual structure and set of conditions. This is clearly an ad hoc approach.

Nearwake stabilizers and fairings. Radial fins that extend along the length of the cylinder have been tested successfully to suppress vortex-excited oscillations [25] in line with the flow. The fins typically are 10 percent of the diameter of the cylinder and are fitted over about 20 percent of the cylinder's length at 45° from the front stagnation point. Such a device is effective only for small variations in the angle of the approach flow. These radial fins also induce a steady side, or lift, force. A streamlined wake fairing that is fitted to a cylinder prevents the formation of strong vortices and has been employed successfully in deep water [24]. However, the fairing must be free to rotate in order to accommodate changes in the direction of the approach flow. Otherwise large bending moments are induced.

Grant and Patterson [24] describe in detail the design, testing and installation of a rotatable fairing for a 610 mm (24 in.) diameter drilling riser that was required to operate in 152 m (500 ft) of water with surface currents of 8 kts. The fairing extended about 2 diameters downstream into the wake of the riser. Flag-type tail fairings were developed for use in the pile installation operations at the Cognac platform site [12].

5.2 A Comparison of Suppression Effectiveness.

Every and King [17, 26, 27] have conducted an extensive program of laboratory experiments to study the effectiveness and optimum configuration of helical strake windings, shrouds, and slats. Some typical examples of their results are shown in Figs. 14 and 15. There the cross flow responses of a bare cylinder and a cylinder fitted with a helically-wound, optimum strake winding are shown. The strake

with a 10 percent projection was fitted over the entire length of the cylinder. For this particular case the reduced damping of the cylinder was very low ($k_s = 0.44$, see the Appendix) and the peak cross flow oscillations were typical of cylinders in water [3,5]. The strake winding was effective in reducing the oscillations to about 10 percent of the bare cylinder values, but it did not completely suppress the oscillatory motion. The vibrations of the strake-wound cylinder were considerably more erratic and random than were the regular, locked-on vibrations of the bare cylinder. Virtually identical results were obtained when the winding extended only over half the cylinder's length.

The conclusions and recommendations of Every and King's study are instructive to potential users of vortex suppression devices. The effectiveness of the various devices was somewhat dependent upon the reduced damping; at low values of k_s the most effective device was the helical strake with a 10 percent projection. The vertical slat array was more effective at large reduced damping, and at $k_s = 3.6$ the vibration displacement was reduced to 5 percent of the bare cylinder value. The shroud device with a 20 to 30 percent open area generally was less effective than either the strake or slat spoilers in that the cross flow displacement was reduced to only 30 percent of the maximum bare cylinder value.

A full-scale drill pipe was fitted with the optimum strake winding and the vibrations were reduced to tolerable levels that allowed drilling at sea to recommence [27]. The strake was recommended because of its relative ease of installation and more generally known characteristics as compared to the vertical slat vortex spoiler. However, the latter was considered to be promising for future applications. Figure 16 shows a photograph of the pipe deployed in the water with a 10 percent helical strake winding made of T-section plastic strip. Prior to the application of the strake winding there had been two fatigue failures of similar pipes. These failures resulted in approximately $5 million in losses.

The choice of any suppression device must take into account the increased steady drag due to the configuration of the device. For example, the strake drag coefficient is $C_D = 1.1$ to 1.3 in the critical range of Reynolds numbers where the bare cylinder $C_D = 0.5$ to 0.6. Though the steady drag is increased substantially, and the steady component of stress on the cylindrical member also in turn is increased, the stress amplification is not nearly as severe as is the case if the structure oscillates due to

vortex shedding. Then there are large oscillatory stresses superimposed upon the steady stress contribution that is caused by the amplified steady deflections and bending moments that are discussed in Section 3 of this report.

It is important to emphasize once again that most effective solutions to the problem of suppressing vortex-excited oscillations are ad hoc in nature and that it is risky to apply a successful result for one installation to other situations. This is especially true in the case of the OTEC cold water pipe, since no suppression device has been tested or employed at the large Reynolds numbers (Re = 10^7 to 10^8) that are characteristic of a full-scale pipe. The Reynolds number of the drill pipe shown in Fig. 16 is about 10^5, somewhat lower than the applicable range of the OTEC cold water pipe.

The resonant, cross flow strumming vibrations of marine cables also sometimes cause severe problems. The suppression of these vibrations has been dealt with effectively, though with the usual penalties of increased drag, etc. Complete and up-to-date discussions of strumming problems and their solution are given in recent reports by Hafen and Meggitt [33], Kline, Nelligan and Diggs [34], Vandiver and Pham [35], and by Kline, Brisbane and Fitzgerald [36]. Again, solutions to the strumming suppression problem for marine cables are ad hoc in nature as well because the precise suppression mechanisms of the various devices are not well understood.

6. SUMMARY

6.1 General Conclusions and Recommendations.

It now is possible to make a reasonably accurate prediction of the likelihood of vortex-induced vibrations and the resulting amplitudes of a structure such as the OTEC cold water pipe. This capability is based upon work that is described here and in the published literature [3,5]. The steady drag force can be evaluated with reasonable accuracy using a method described in this report. Extensive comparisons between predictions and experimental measurements of the steady deflection due to the drag on a vibrating structure are given here and by Every, King and Griffin [17]. Thus it now is possible to predict the hydrodynamic loading and material stresses with some confidence.

This report also describes several methods of reducing the oscillations, and hence loads, due to vortex-induced oscillations by means of clamp-on spoiler devices. None of the proposed methods have been adequately tested on cylinders that are free to oscillate in the OTEC cold water pipe range of Reynolds number. The nonlinear interaction between the cylinder motion and the vortex shedding dictates that further testing be conducted to evaluate the performance of the various devices.

Additional experiments are required to add to the data on the increase in drag coefficient with oscillation amplitude. However, this report and a related paper [17] set out a method for making preliminary assessments which are adequate for most practical cases.

6.2 Steady Hydrodynamic Drag Effects in OTEC CWP Design.

The previous sections of this report and a previous report [5] have summarized the state of the art for predicting the susceptibility of marine structures to vortex-excited oscillations. The procedures to be followed in the design process are summarized in Section 3 and the Appendix of this report. All of the methods described can be applied in principle to the design of the OTEC cold water pipe. Extensive comparisons have been made with measured drag-induced deflections of flexible cantilever beams in water to verify the design method that is presented in this report.

The results generally are applicable to the OTEC cold water pipe if a preliminary assessment is desired and the hydrodynamic drag coefficient for the stationary pipe is known. Additional stationary and vibrating cylinder drag coefficient data are required if the method is to be applied with full confidence at the higher Reynolds numbers (Re = 10^6 and above) that are relevant to the full-scale pipe.

6.3 Suppression of Vortex-Excited Oscillations — Considerations in OTEC CWP Design.

Section 5 of this report provides an up-to-date survey of available means to suppress vortex-excited oscillations. Several methods of reducing the oscillations by means of clamp-on devices are discussed. It is possible to reduce the vortex-induced vibration levels and hydrodynamic loads to acceptable levels with a number of the devices. An example is given of the successful use of a helical wrap or strake vortex spoiler in a full-scale marine application at a Reynolds number of 10^5. It is important to emphasize once again, however, that most of the effective devices have been developed by ad hoc methods and that the candidate devices for each individual application should be carefully tested to provide a practical and economical solution. No vortex supression device has been tested or employed at large Reynolds numbers (Re = 10^6 and above) that characterize the full-scale OTEC cold water pipe. Thus particular care must be taken at this stage of development before any one type of device is recommended for use in OTEC cold water pipe applications.

7. REFERENCES

1. M.G. Hallam, N.J. Heaf and L.R. Wootton, "Dynamics of Marine Structures," Construction Industry Research and Information Association (CIRIA) Report UR8, London, 1978.

2. R.D. Blevins, *Flow-Induced Vibrations*, Van Nostrand Reinhold: New York, 1977.

3. R. King, "A Review of Vortex Shedding Research and Its Application," Ocean Engineering, Vol. 4, 141-171, 1977.

4. T. Sarpkaya, "Vortex-Induced Oscllations, A Selective Review," Trans. of ASME, Journal of Applied Mechanics, Vol. 46, 241-258, 1979.

5. O.M. Griffin, "OTEC Cold Water Pipe Design for Problems Caused by Vortex-Excited Oscillations," NRL Memorandum Report 4157, March 1980; see also Ocean Engineering, Vol. 8, 129-209, 1981.

6. N. Hogben, B.L. Miller, J.W. Searle and G. Ward, "Estimation of Fluid Loading on Offshore Structures," Proc. of the Institution of Civil Engineers, Vol. 63, 515-562, 1977.

7. T. McGuinness and R. Scotti, "OTEC Cold Water Pipe Program Status," Offshore Technology Conference Preprint OTC 3685, May 1980.

8. O.M. Griffin and J.G. Giannotti (eds.), "Ocean Engineering for OTEC," ASME: New York, February 1980.

9. Science Applications Inc., "OTEC Modular Experiment Cold Water Pipe Concept Evalutation" Technical Report SAI-063-80R-008-LA, March 1979.

10. O.M. Griffin and S.E. Ramberg. "On vortex strength and drag in bluff body wakes," Journal of Fluid Mechanics, Vol. 69, 721-728, 1975.

11. R.A. Skop, O.M. Griffin and S.E. Ramberg, "Strumming Predictions for the Seacon II Experimental Mooring," Offshore Technology Conference Preprint OTC 2884, 1977.

12. F.J. Fischer, W.T. Jones and R. King, "Current-Induced Oscillations of Cognac Piles During Installation--Prediction and Measurement," in E. Naudascher and D. Rockwell (eds.) *Proc. Symposium on Practical Experiences with Flow-Induced Vibrations,* Springer-Verlag: Berlin, 570-581, 1980.

13. R. King, "Model Tests of Vortex Induced Motion of Cable Suspended and Cantilevered Piles for the Cognac Platform," BHRA Report RR 1453, January 1978.

14. G. Grimminger, "The Effect of Rigid Guide Vanes on the Vibration and Drag of a Towed Circular Cylinder," David Taylor Model Basin Report 504, April 1945.

15. D.W. Dareing and T. Huang, "Marine Riser Vibration Response Determined by Modal Analysis," ASME Paper 78-Pet-12, November 1978; see also Petroleum Engineer International, Vol. 52, 56-76, May 1980.

16. R.E.D. Bishop and D.C. Johnson, *Mechanics of Vibration,* Cambridge University Press: Cambridge, 1960; Chapter 7.

17. M.J. Every, R. King and O.M. Griffin, "Hydrodynamic Loads on Flexible Marine Structures due to Vortex Shedding," ASME Paper 81-WA/FE - 24, November 1981.

18. R.D. Peltzer and D.M. Rooney, "The Effects of Upstream Shear and Surface Roughness on the Vortex Shedding Patterns and Pressure Distributions Around A Circular Cylinder in Transitional Re Flows," Virginia Polytechnical Institute and State University Report VPI-Aero-110, April 1980.

19. F.D. Deffenbaugh, "Experimental Investigation of the Motion of a 70 ft. PVC Cold Water Pipe," TRW Report 35892-6001-UE-00, March 1980.

20. S. Taylor, W. Shih and D. Hove, "An OTEC Cold Water Pipe Hydroelastic Response Experiment," Science Applications Inc. Report SAI-063-80R-047-LA, July 1979.

21. V. Griffith, J. Ryken, and W. Dukes, "Cold Water Pipe (CWP) Feasibility Test Final Report," Bell Aerospace TEXTRON Report 2831-928002, February 1979.

22. O.M. Griffin, S.E. Ramberg, R.A. Skop, D.J. Meggitt and S.S. Sergev, "The Strumming Vibrations of Marine Cables: State of the Art," Naval Civil Engineering Laboratory, Port Hueneme, CA, Technical Note N-1608, May 1981.

23. O.M. Griffin, J.H. Pattison, R.A. Skop, S.E. Ramberg and D.J. Meggitt, "Vortex-Excited Vibrations of Marine Cables," Proc. of ASCE, Journal of the Waterway, Port, Coastal and Ocean Division, Vol. 106, No. WW2, 183-204, 1980.

24. R. Grant and D. Patterson, "Riser Fairing for Reduced Drag and Vortex Suppression," Offshore Technology Conference Preprint OTC 2921, 1977.

25. R. King M.J. Prosser and R.L.P. Verley, "The Suppression of Structural Vibrations Induced by Currents and Waves," B.O.S.S. Conference Proceedings (Trondheim), Vol. I, 263-283, 1976.

26. M.J. Every and R. King, "Suppressing Flow Induced Vibrations—An Experimental Study of Clamp-On Devices," BHRA Fluid Engineering Report RR 1576, November 1979.

27. M. Every and R. King, "Drill pipe vibration problem whipped in strong English Channel currents," Oil and Gas Journal, 93-06, June 2, 1980.

28. M.M. Zdravkovich, "Review and Classification of Various Aerodynamic and Hydrodynamic Means for Suppressing Vortex Shedding," J. of Industrial Aerodynamics and Wind Engineering, Vol. 7, 145-189, 1981.

29. R.B. Dean and L.R. Wootton, "An Analysis of Vortex Shedding Problems in Offshore Engineering," Atkins Research and Development Report No. 77/14, Epsom (UK), 1977.

30. ----------, "STARSTRAKE for the Suppression of Vortex Shedding from Circular Cylinders in Tides and Currents," Fathom Oceanology Ltd, Test Report 6.841 T, October 1978.

31. L.R. Wootton, M.H. Warner, R.N. Sainsbury and D.H. Cooper, "Oscillations of Piles in Marine Structures," Construction Industry Research and Information Association (CIRIA) Report 41, London, 1972.

32. H.Y. Wong, "An aerodynamic means of suppressing vortex excited oscillation," Proceedings of the Institution of Civil Engineers, Vol. 63, 693-699, 1977.

33. R.E. Hafen and D.J. Meggitt, "Cable Strumming Suppression," Civil Engineering Laboratory, Naval Construction Battalion Center, Technical Note N-1499, September 1977.

34. J.E. Kline, J.J. Nelligan and J.S. Diggs, "A Survey of Recent Investigations into the Nature of Cable Strumming, its Mechanism and Suppression," MAR Inc. Technical Report 210, July 1978.

35. J.K. Vandiver and T.P. Pham, "Performance Evaluation of Various Strum Suppression Devices," MIT Ocean Engineering Department Report 77-2, March 1977.

36. J.E. Kline, A. Brisbane and E.M. Fitzgerald, "Cable Strumming Suppression," MAR Incorporated Technical Report 249, October 1980.

8. APPENDIX: METHODS FOR ESTIMATING THE SUSCEPTIBILITY OF BLUFF BODIES TO VORTEX-EXCITED OSCILLATIONS.

8.1 A General Assessment.

Design procedures and prediction methods for analyzing the vortex-excited oscillations of structures have been developed only since the mid—1970's. Previously a reliable experimental data base and accurate characterization of the phenomenon were relatively unavailable, and it only has been since marine construction has moved into deeper water and more harsh operating environments that the need for sophisticated design procedures has arisen. The need to design slender, flexible structures against problems due to vortex shedding in the atmospheric environment also has spurred renewed efforts to develop new wind engineering design procedures. It should be emphasized, however, that reliable data are available only at subcritical Reynolds numbers. The design procedures that generally are available have been discussed recently in two related reports [5,22].

All of the methods developed thus far are in common agreement and point out that the following parameters determine whether large-amplitude oscillations will occur:

- The logarithmic decrement of *structural* damping, δ ;
- The reduced velocity, $V/f_n D$;
- The mass ratio, $m_e/\rho D^2$.

Here m_e is the effective mass of the structure which is defined as

$$m_e = \frac{\int_0^l m(x) y^2(x)\,dx}{\int_0^l y^2(x)\,dx} \tag{A1}$$

where m (x) is the cylinder mass per unit length including internal water or other fluid and the added mass, joints, sections of different material, etc.;

$y(x)$ is the modal shape of the structure along its length;

L is the overall length of the structure, measured from its termination,

h is the water depth.

It should be noted here that many of these methods were developed originally for structural members that pierced the water surface, hence the length L was greater that the depth h. The effective mass m_e then defines an equivalent structure whose vibrational kinetic energy is equal to that of the real structure.

As described in Refs. 3, 5 and 22, the mass parameter and the structural damping can be combined as:

$$k_s = \frac{2m_e\delta}{\rho D^2} \text{ or } \frac{\zeta_s}{\mu} = 2\pi \mathrm{St}^2 k_s , \tag{A2}$$

which in both forms are called the reduced damping. The reduced damping k_s is the ratio of the actual damping force (per unit length) and $\rho f_n D^2$, which can be viewed as an inertial force. Available results also suggest criteria for determining the critical incident flow velocities for the onset of vortex-excited motions. These critical velocities are

$$V_{\text{crit}} = (f_n D) V_{r,\text{crit}} \tag{A3}$$

where $V_{r,\text{crit}} = 1.2$ for in line oscillations and $V_{r,\text{crit}} = 3.5$ for cross flow oscillations at Reynolds numbers greater than 5×10^5. For Reynolds number below 10^5, $V_{r,\text{crit}} = 5$.

It was noted above that the peak cross flow displacement amplitude is a function primarily of a response or reduced damping parameter when the damping is small and $\zeta_s = \delta/2\pi$. The importance of the reduced damping follows directly from the resonant force and energy balances on the vibrating structure. Moreover, the relation between $Y_{MAX}(Y = \bar{Y}/D)$ and k_s or ζ_s/μ holds equally well for flexible cylindrical structures with normal mode shapes given by $\psi_i(z)$,, for the i th mode. If the cross flow displacement (from equilibrium of a flexible structure is written as

$$y_i = Y\psi_i(z)\sin\omega t$$

at each spanwise location z, the peak placement is scaled by the factor

$$Y_{EFF,MAX} = YI_i^{1/2} / \mid \psi_i(z) \mid_{MAX} = Y_i/\gamma_i \tag{A4}$$

In this equation

$$I_i = \frac{\int_0^L \psi_i^4(z)\, dz}{\int_0^L \psi_i^2(z)\, dz}$$

and

$$\gamma_i = \frac{\mid \psi_i(z) \mid_{MAX}}{I_i^{1/2}}$$

which are derived from considerations based on several related versions of the so-called "wake oscillator" formulation for predicting vortex-excited oscillations. Typical values of γ_i, ψ_i and I_i are tabulated in Refs. 5 and 22.

An incresase in the reduced damping results in smaller amplitudes of oscillation and at large enough values of ζ_s/μ or k_s the vibratory motion becomes negligible. Reference to Fig. 17 suggests that oscillations are effectively suppressed at $\zeta_s/\mu > 4$ (or $k_s > 16$). Cylindrical structures in water fall well toward the left-hand portion of the figure. The measurements of in line oscillations in water have shown that vortex-excited motions in that direction are effectively negligible for $k_s > 1.2$. The results obtained by Dean, Milligan and Wootton [37], King [13] and others shown in Fig. 17 indicate that the reduced damping can increase from $\zeta_s/\mu = 0.01$ to 0.5 (a factor of 50) and the peak-to-peak displacement amplitude is decreased only from 2 or 3 diameters to 1 diameter (a nominal factor of only two or three). At the small mass ratios and structural damping ratios that are typical of light, flexible structures in water, hydrodynamic effects predominate and it is difficult to reduce or suppress the oscillations by changing the mass and damping of the structure.

8.2 Step-by-Step Procedures.

A sequence of procedures for determining the deflections that result from vortex-excited oscillations have been proposed by several groups, and these procedures are summarized in Refs. 5 and 22. The steps to be taken generally should follow the sequence:

- Compute/measure vibration properties of the structure (natural frequencies or periods, normal modes and modal scaling factors, etc.);

- Compute Strouhal frequencies and test for critical velocities, (in line and cross flow), based upon the incident flow environment;

- Test for reduced damping, based upon the structural damping and mass characteristics of the structure.

If the structure is susceptible to vortex-excited oscillations, then:

- Determine vortex-excited unsteady displacement amplitudes and corresponding steady-state deflections based upon the steady drag amplification that accompanies the oscillations;

- Determine new stress distributions based upon the new steady-state deflection and the superimposed mode shape caused by the unsteady forces, displacements and accelerations due to vortex-shedding;

- Assess the severity of the amplified stress levels relative to fatigue life, critical stresses, etc.

These general procedures are discussed in detail in Ref. 5 where several practical design problems relevant to the OTEC cold water pipe also are given as examples. The sequence to be followed in assessing the drag-induced deflections is given in Fig. 4 of this report.

Table 1 — Physical Properties of the Cognac Pile Hydroeleastic Modelling Experiments From King [13]

Physical Property Full Scale/Model	Scale Factor, Value	Actual Model
Length	168	2.17 ft
Diameter D	168	0.042 ft
Stiffness $3EI/L^3$	168	2.02 lb_f/ft
Structural mass/unit length m	$(168)^2$	0.041 lb_m/ft
Logarithmic decrement δ	1	0.063
In-air natural frequency f_{na}	1/168	8.75 Hz

Table 2 — Static Deflection and Steady Drag Amplification Due to Vortex-Excited Oscillations

Measurements from King [13]; Every, King and Griffin [17]
Predictions from Eqs. (4), (8), (13); present study.

Tip deflection, Y_s (Diameters) $= KC_{D0}\, 0.125\, A_1 + B_1A_2\,(1 + B_2) - 0.048\, B_1A_2B_2$

From Table 1, $K = 3.14\, V^2$

Drag amplification, $C_D/C_{D0} = A_1 + B_1A_2\, 1 + B_2 - \frac{2}{\pi}\, B_1A_2B_2$

Bending moment amplification, $M/M_0 = A_1 + B_1A_2\, 1 + B_2 - 0.462\, B_1A_2B_2$

Case One:

$A_1 = 0.54,\ B_1 = 0.88,\ A_2 = \text{St}\ V_r^{-1} = 0.71,\ B_2 = 2\bar{Y}/D = 2.9,\ V = 1.08$ ft/sec,

$C_{D0} = 1.2,\ \text{SG} = 3.5$

$Z_s = 1.2$ *Diameters (Predicted)* $Z_s = 1.3$ *Diameters (Measured, Fig. 2)*

$C_D/C_{D0} = 1.82,\ M/M_0 = 2.14$ *(Predicted)*

Case Two:

$A_1 = 0.54,\ B_1 = 0.88,\ A_2 = 0.83,\ B_2 = 2.5,\ V = 0.96$ ft/sec, $C_{D0} = 1.2,\ SG = 3.5$

$Z_s = 1$ *Diameter (Predicted)* $Z_s =$ *Diameter (Measured, Fig. 2)*

$C_D/C_{D0} = 1.93,\ M/M_0 = 2.50$ *(Predicted)*

Case Three:

$A_1 = 0.54,\ B_1 = 0.88,\ A_2 = 0.67,\ B_2 = 2.5,\ V = 1.38$ ft/sec, $C_{D0} = 1.2,\ SG = 2.0$

$Z_s = 1.83$ *Diameters (Predicted)* $Z_s = 1.9$ *Diameters (Measured Fig. 2)*

$C_D/C_{D0} = 1.67,\ M/M_0 = 1.92$ *(Predicted)*

Table 3 — TRW Experimental Program:
At-Sea Tests of a 21.4 m (70 ft) PVC Cold Water Pipe†
Pipe Diameter D = 0.22 m (8.6 in.)

Run	V	f	n	$V_r = V/fD$	
16	2.41 ft/sec (1.43 kt)	0.53 Hz	2	6.3 (n = 2)	Cross flow oscillations at the high flow velocity end of the n = 2 resonance.
17	2.44 ft/sec (1.44 kt)	0.88 Hz	3	3.9 (n = 3), 6.4 (n = 2)	Cross flow oscillations at the low flow velocity end of the n = 3 resonance.

†See TRW Report 35892-6001-UE-00

Notes:

1. The model pipe was filled with water.
2. A bottom weight of W = 1000 lb was attached to the lower end of the pipe. The upper end of the pipe was mounted in a universal joint.
3. The PVC pipe was tuned to undergo resonant cross flow oscillations in the n = 2 mode at a tow speed of 1 kt (1.69 ft/sec).

Table 4 — Vortex-excited Cross Flow Displacement Amplitude Response of Cylindrical Structures.
Legend for Data Points in Fig. 17

Type of cross-section and mounting; medium	
Various investigators, from Griffin [5]:	
Spring-mounted rigid cylinder; air	*○–✖◐
Spring-mounted rigid cylinder; water	◆
Cantilevered flexible circular cylinder; air	⅄
Cantilevered flexible circular cylinder; water	X▽⊕
Pivoted rigid circular rod; air	⊐▲
Pivoted rigid circular rod; water	●
From Dean, Milligan and Wootton; see Ref. 5:	
Spring-mounted rigid cylinder; water	◩
Flexible circular cylinder, L/D = 240; water	◪
From King [13]:	
Cantilevered flexible circular cylinder, L/D = 52 (PVC); water	◴
Cantilevered flexible circular cylinder, L/D = 52 (stainless steel); water	◶

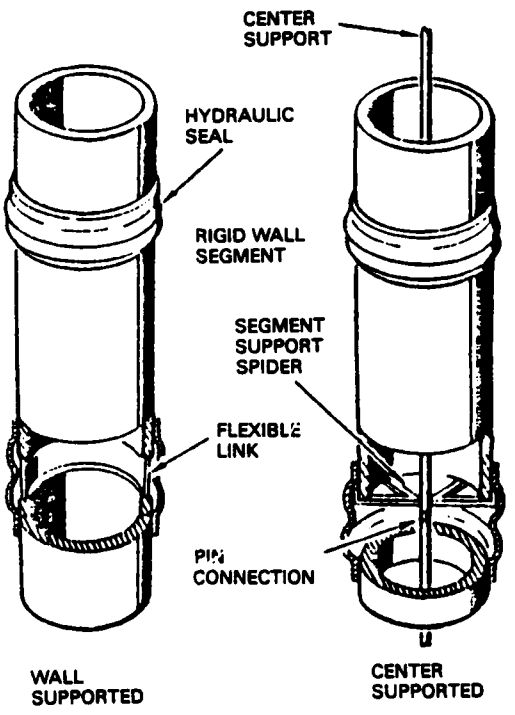

Fig. 1 — Typical rigid-wall OTEC cold water pipe concept (no articulated joints) for a 10/40 MW_e plant

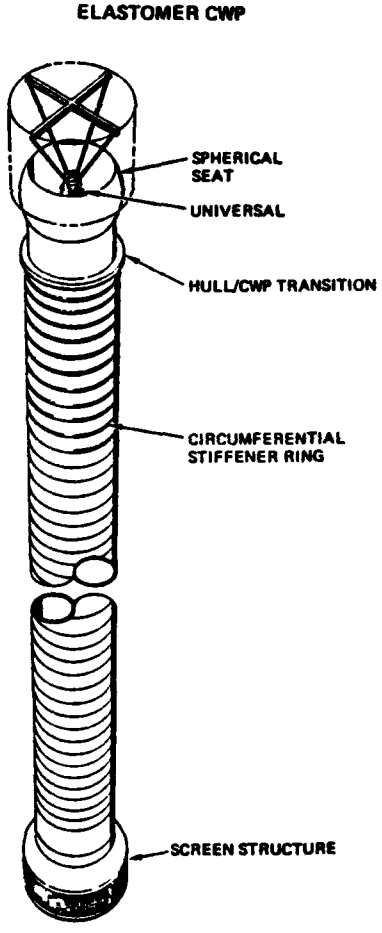

Fig. 2 — Typical compliant-wall OTEC cold water pipe concept (steel cable-reinforced) elastomeric construction) for a 10/40 MW_e plant

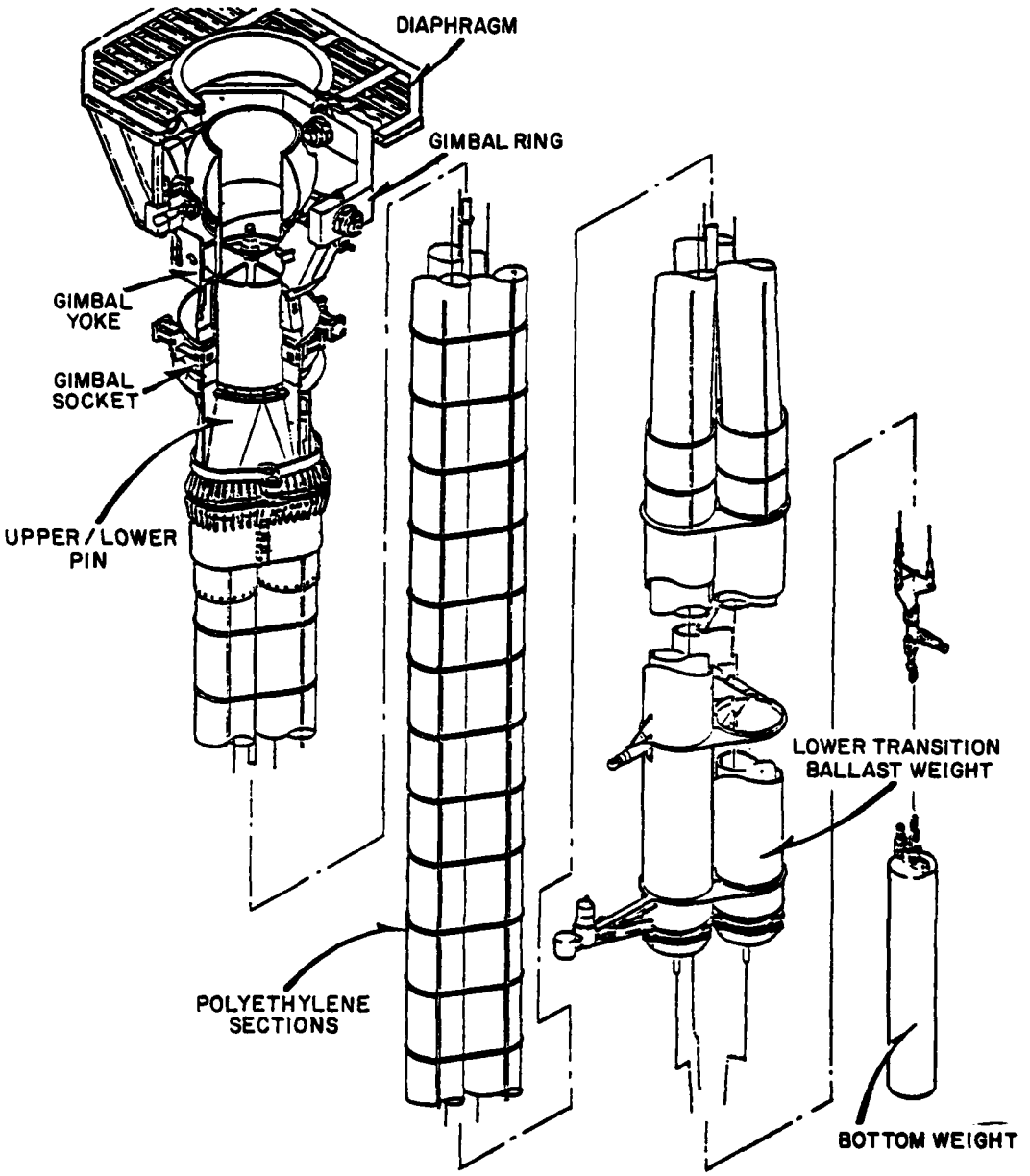

Fig. 3 — A line diagram of the cold water pipe system that has been deployed from the operational test platform OTEC-1.

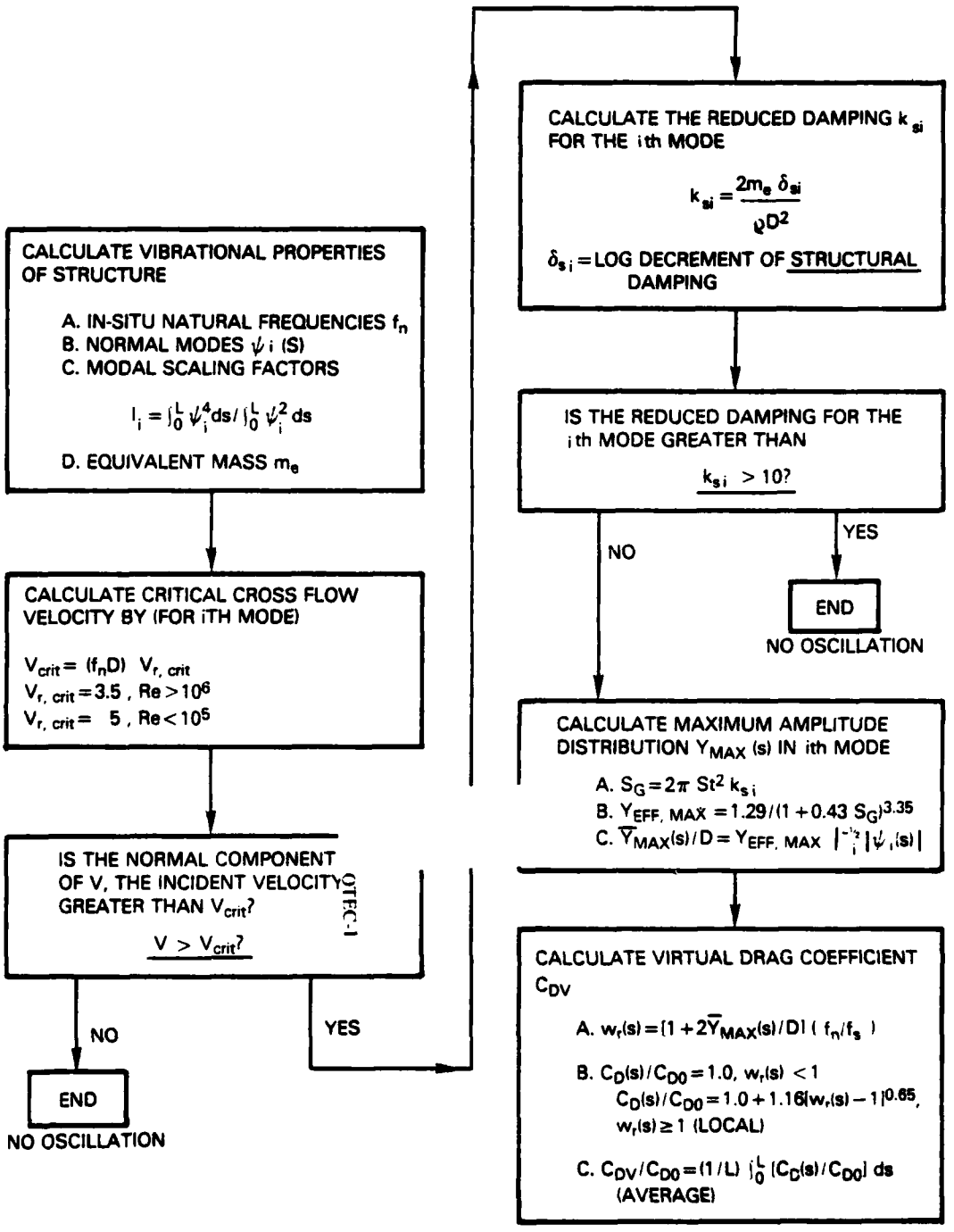

Fig. 4 — Flow diagram of the steps required for the calculations of the steady drag amplification due to resonant vortex-excited oscillations; from Griffin [5].

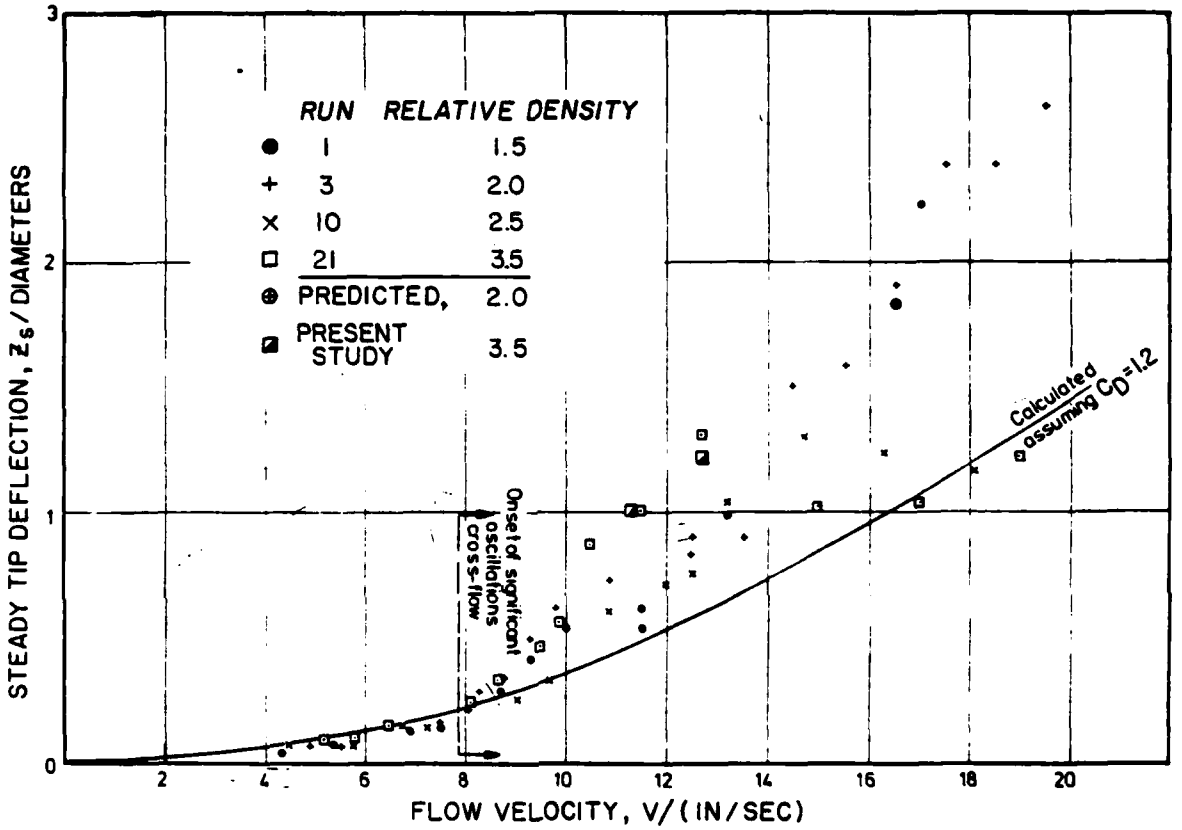

Fig. 5 — Drag-induced steady deflection at the tip of a free-ended cantilever marine pile. The pile was oscillating perpendicular to the incident flow in the resonant response regime shown for water velocities greater than $V = 8$ in./sec; from King [13].

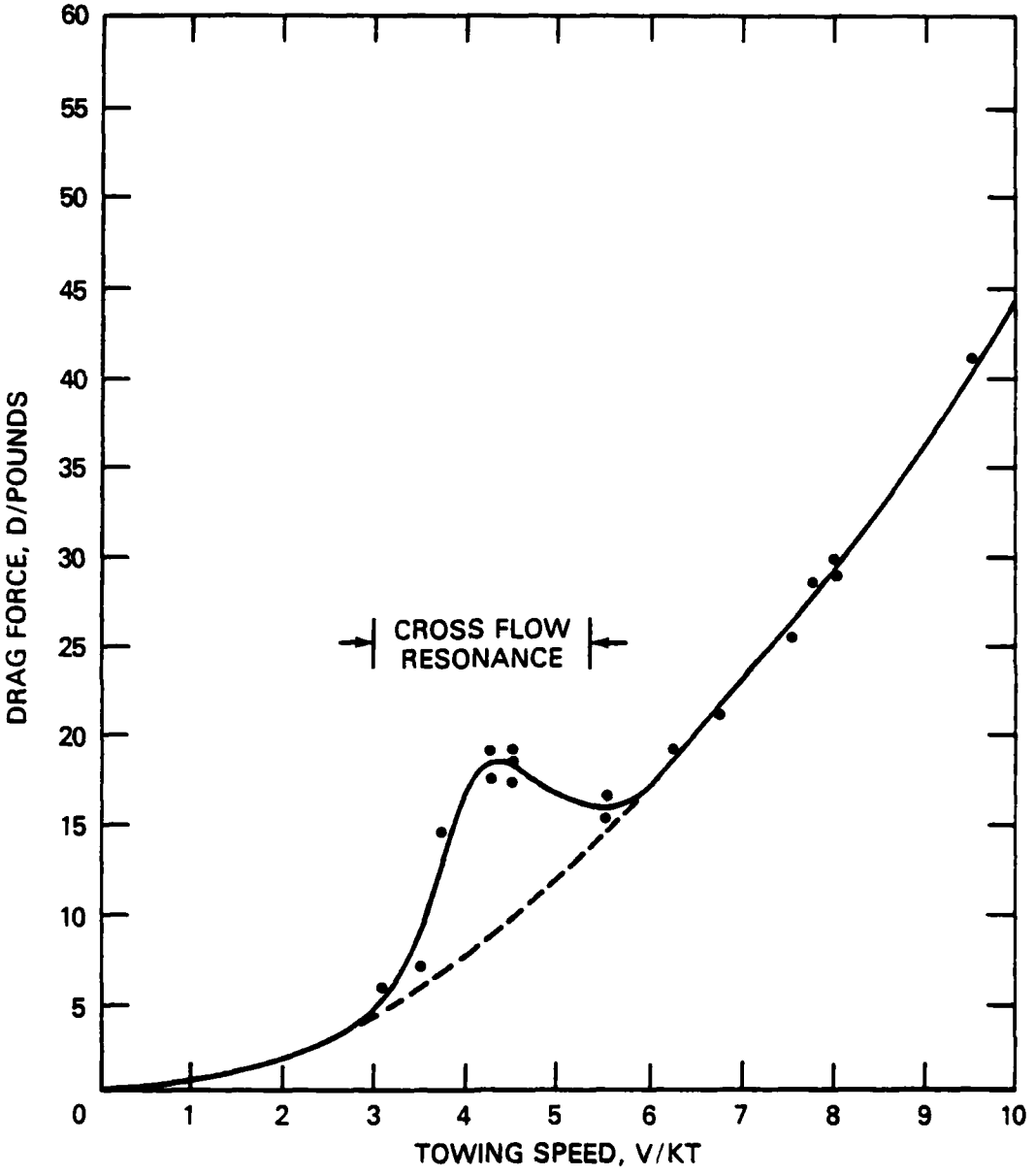

Fig. 6 — Steady drag force measured on a free-ended circular cylinder towed through still water. A clear resonance in the drag due to vortex-excited oscillations perpendicular to the incident flow is shown between relative flow speeds of $V = 3$ and 6 kts; from Grimminger [14].

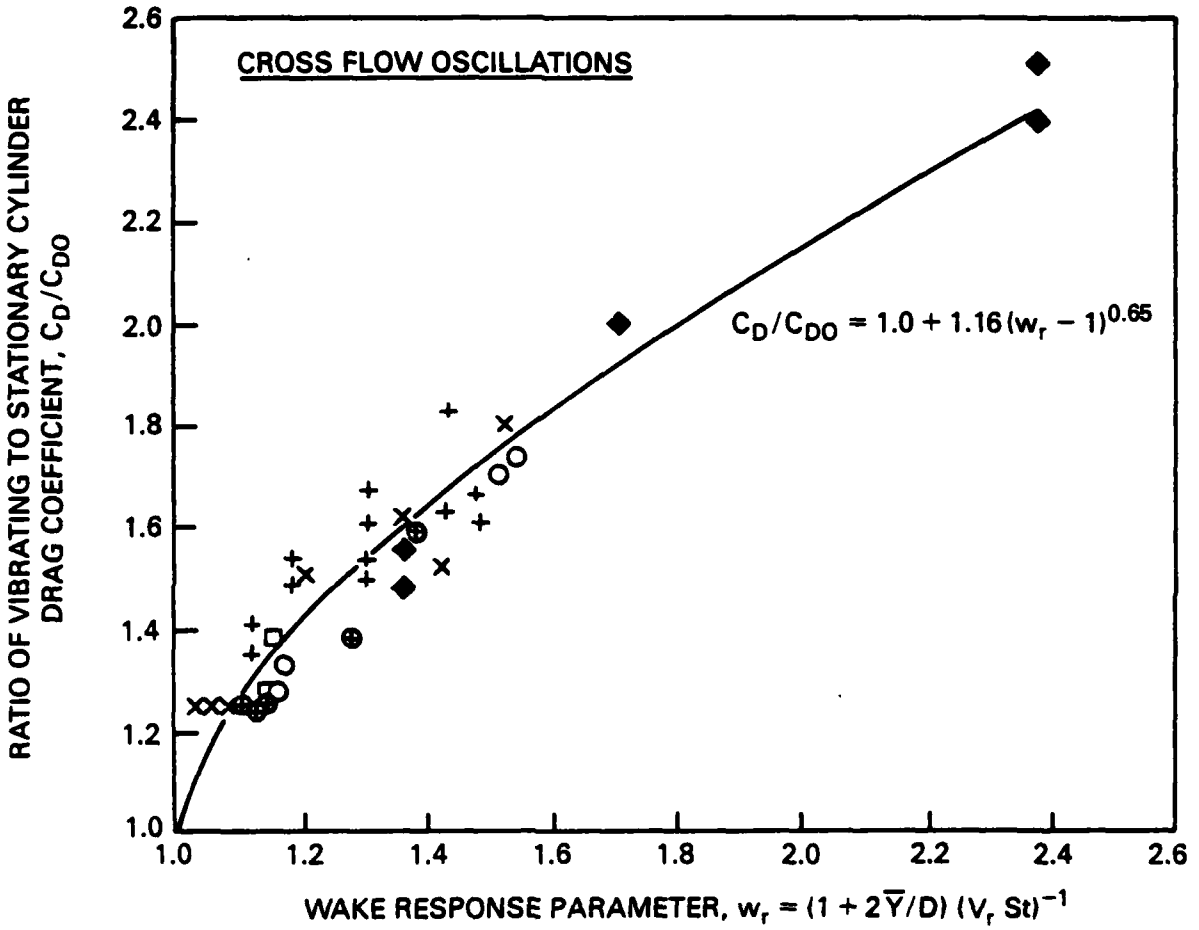

Fig. 7 — The ratio of the steady drag coefficient C_D due to vortex-excited cross flow oscillations and the steady drag coefficient C_{D0} on a stationary circular cylinder plotted against the "wake response" parameter w_r. Here $2\overline{Y}/D$ is the peak-to-peak displacement amplitude (D is the diameter of the cylinder), V_r is the reduced velocity and St is the Strouhal number; from Griffin [5].

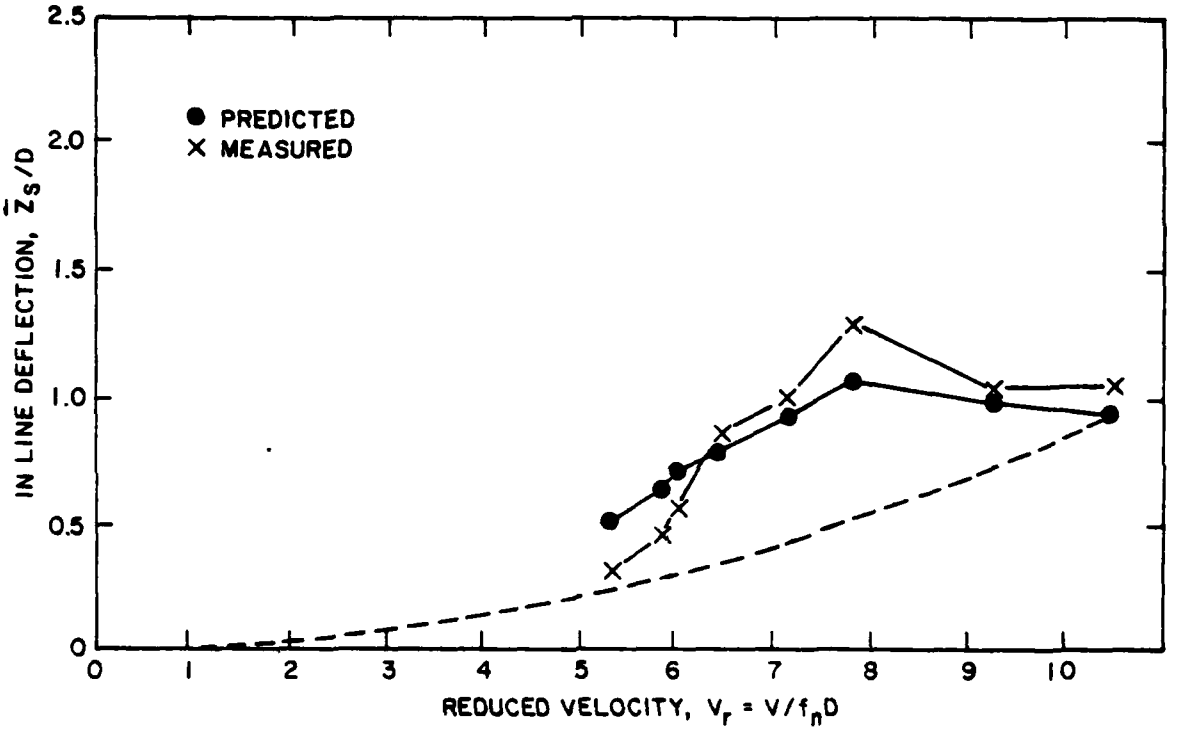

Fig. 8 — The steady tip deflection Z_t of a cantilever beam, predicted by Eq. (8), compared with the measured values for a cylinder of relative density $SG = 3.5$ shown in Fig. 5. The prediction using a constant $C_D = 1.2$ is shown by the dashed line; from Every, King and Griffin [17].

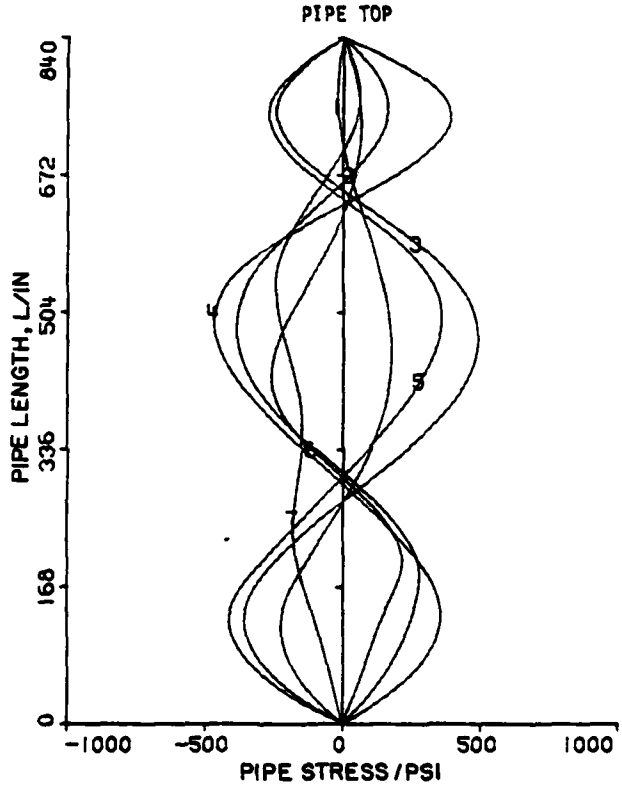

Fig. 9 — Experimental stress history from a grazing test run conducted with the TRW 70 ft long PVC cold water pipe [19]. The individual stress curves were recorded at time intervals of $\Delta t = 1$ sec; the resonance clearly is in the third ($n = 3$) mode.

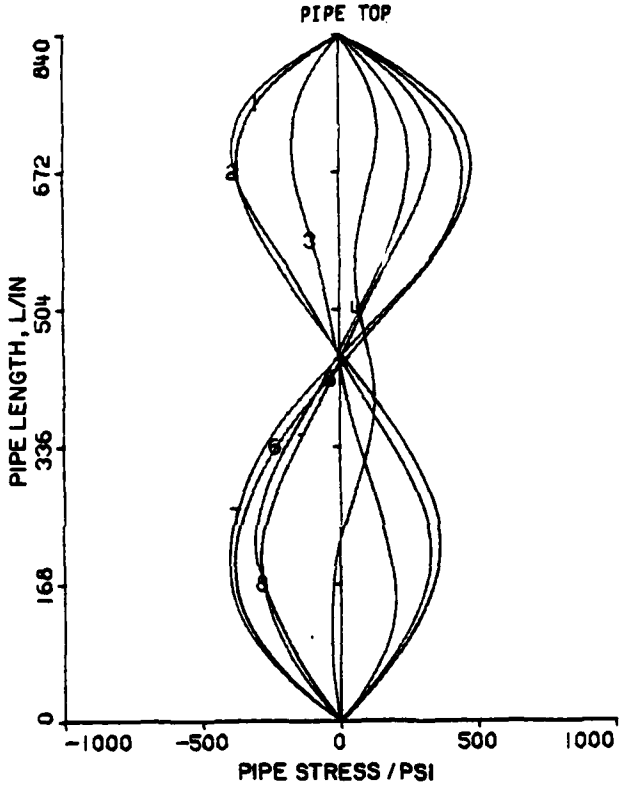

Fig. 10 — Experimental stress history from a grazing test run conducted with the TRW 70 ft long PVC cold water pipe [19]. The individual stress curves were recorded at time intervals of $\Delta t = 0.2$ sec; the resonance clearly is in the second ($n = 2$) mode.

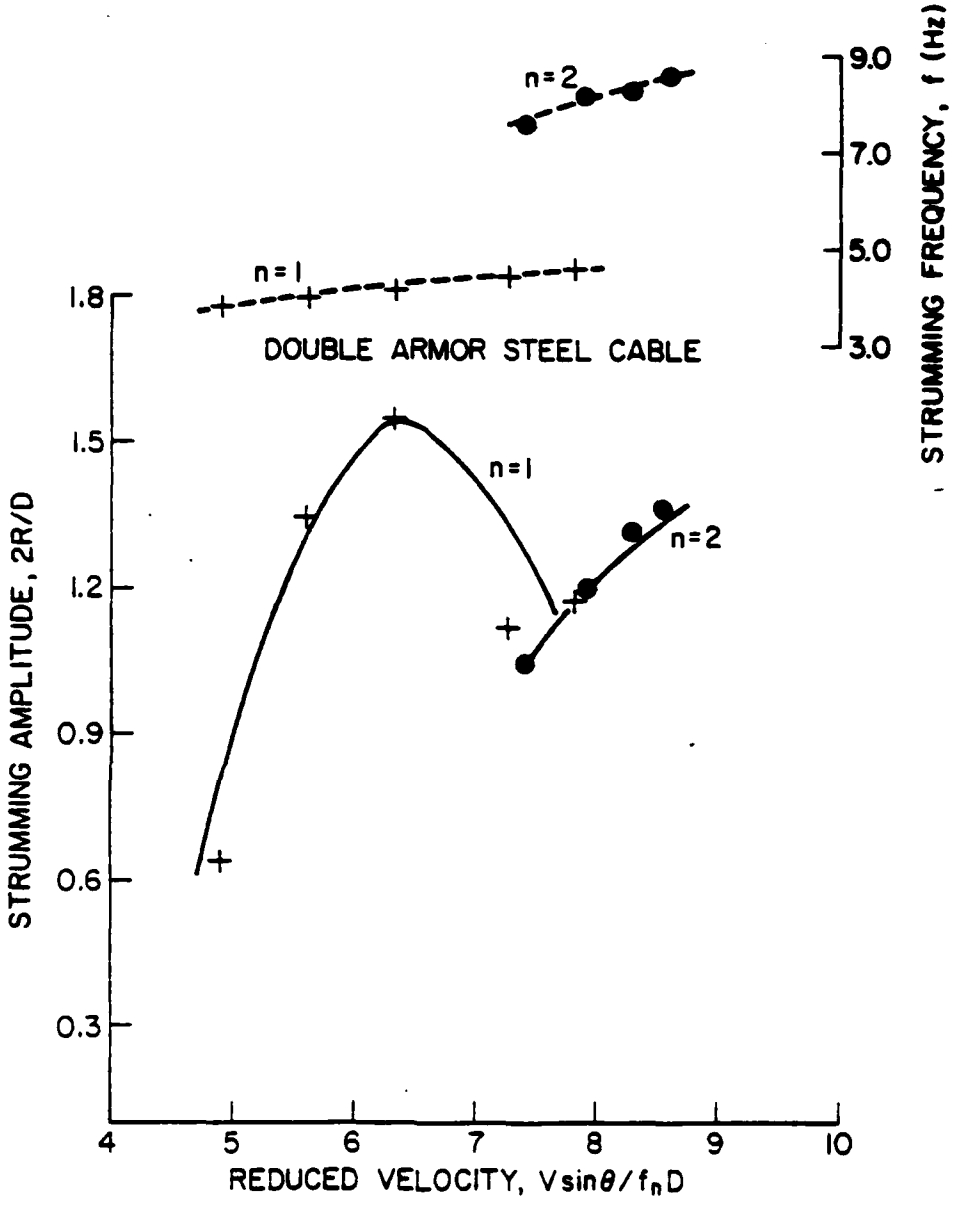

Fig. 11 — Resonant cross flow strumming response (displacement amplitude $2\bar{Y}/D$) of a Double Armor Steel (DAS) marine cable plotted against the incident flow speed (reduced velocity V_r); from Refs. 22 and 23. The cable response is shown in two ($n = 1, 2$) modes with some overlap at the modal boundary.

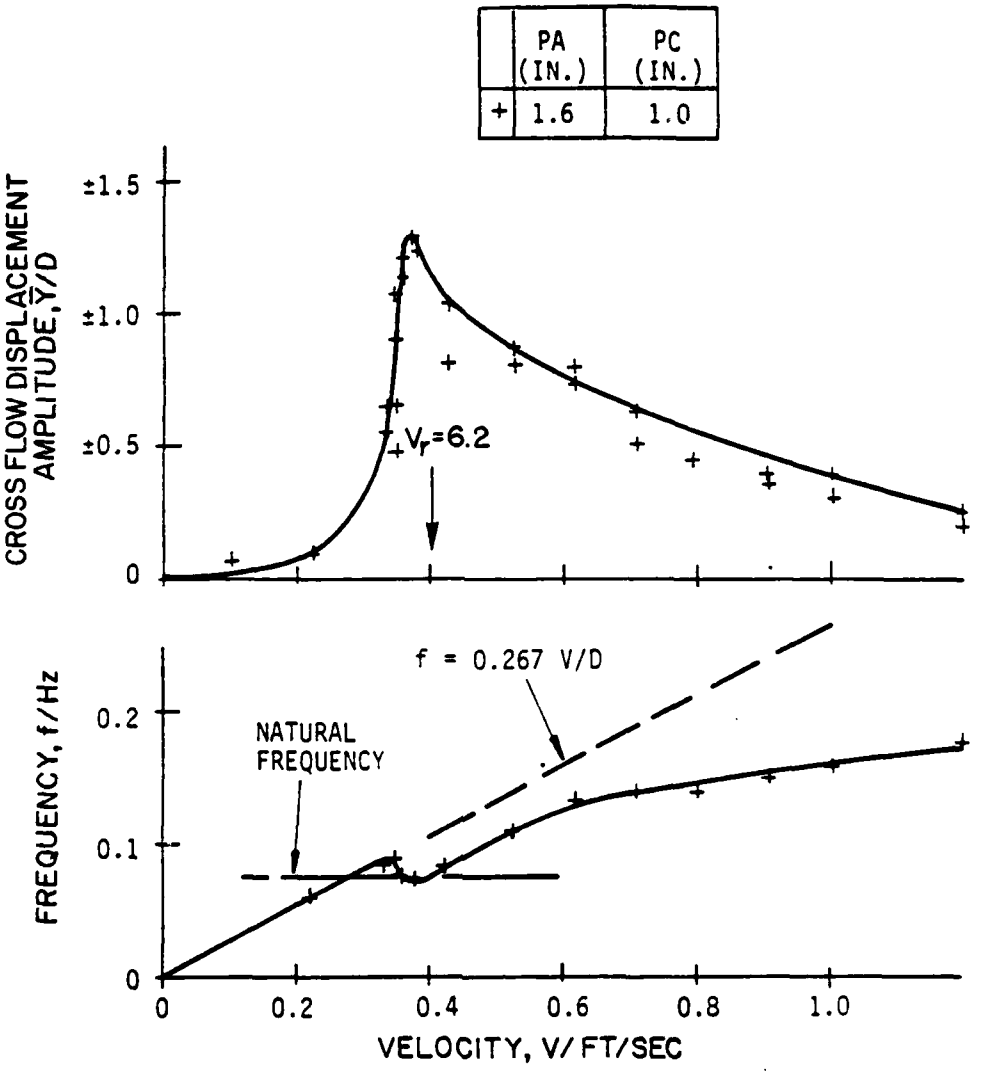

Fig. 12 — Resonant cross flow vortex-excited oscillation (displacement amplitude $\bar{Y}/D$) of an annular compliant-wall cold water pipe model, plotted against the tow speed V; from Ref. 20. The pipe was constructed of urethane-coated nylon fabric to form the pressurized annular configuration.

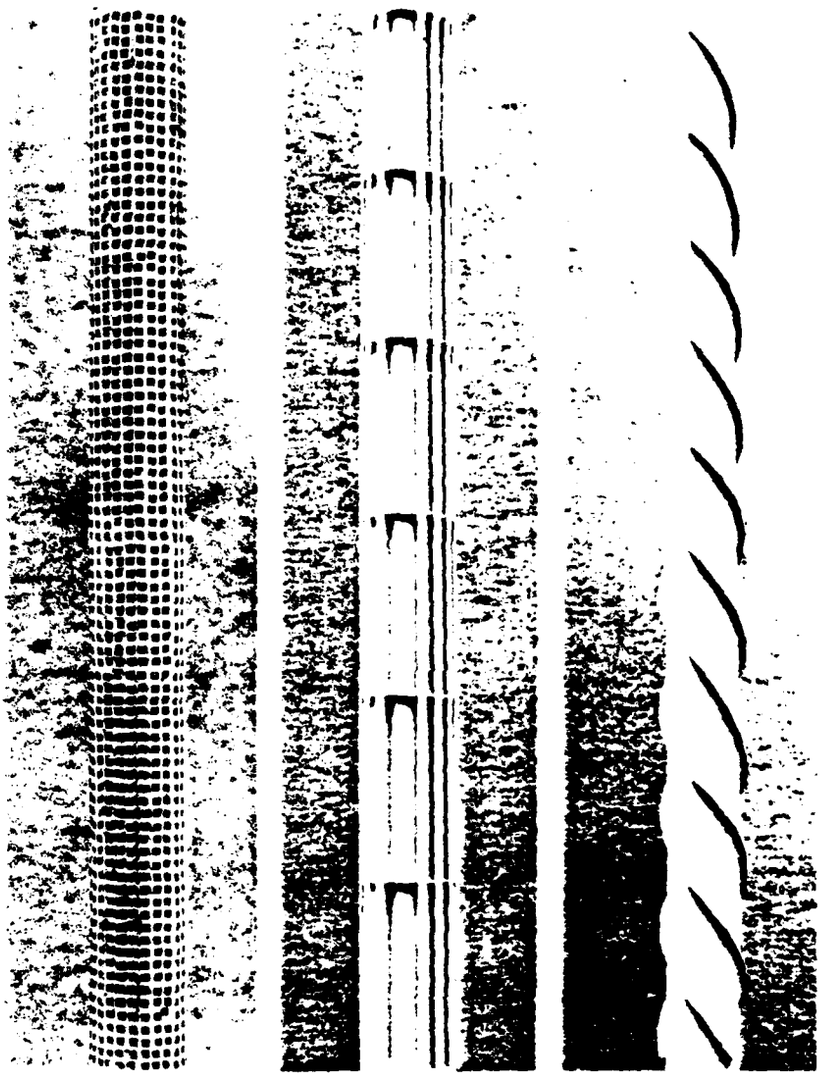

Fig. 13 — Typical devices for suppressing the vortex-excited oscillations of bluff cylindrical structures; from Every and King [26]. Shown in the photographs are a perforated shroud (left), longitudinal slats (center), and a 10% helical strake.

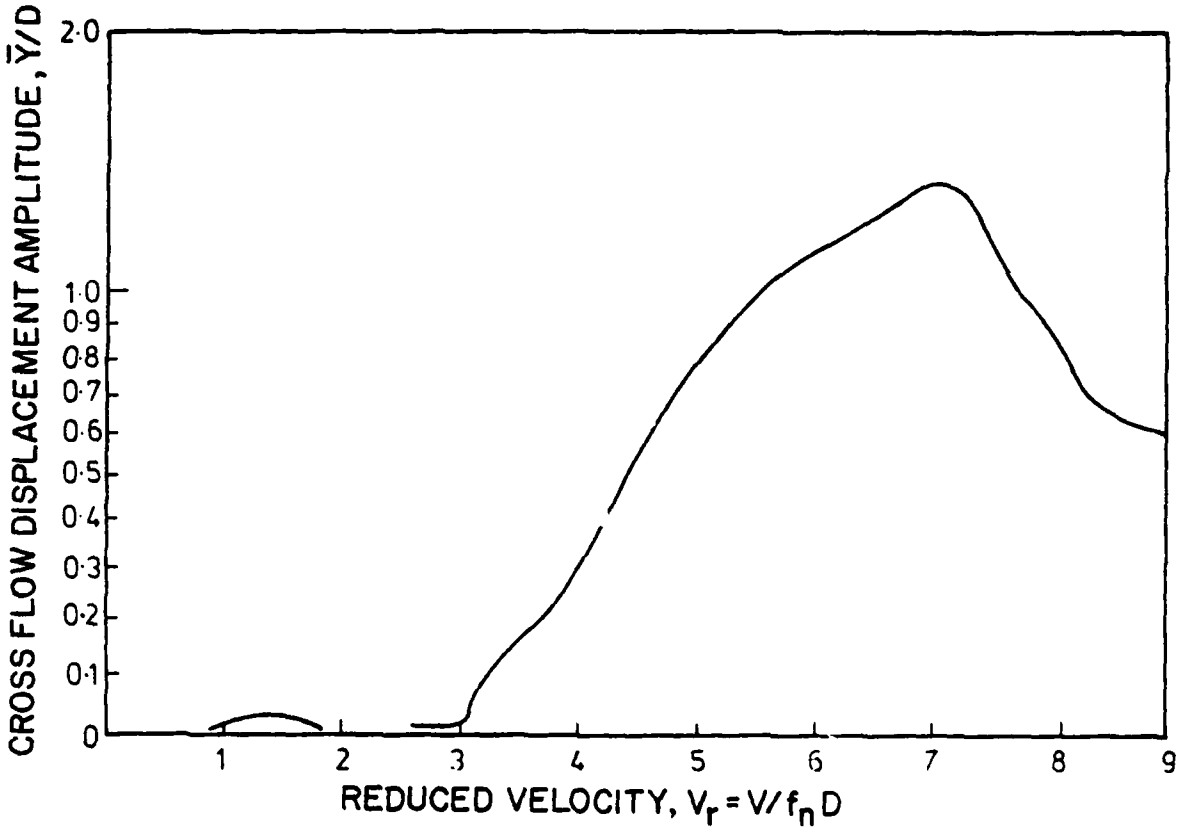

Fig. 14 — The vortex-excited response (displacement amplitude $\bar{Y}/D$) of a bare cylinder plotted against the incident reduced water flow velocity, $V_r = V/f_n D$; from Every and King [26]. Cylinder reduced damping $k_s = 0.44$.

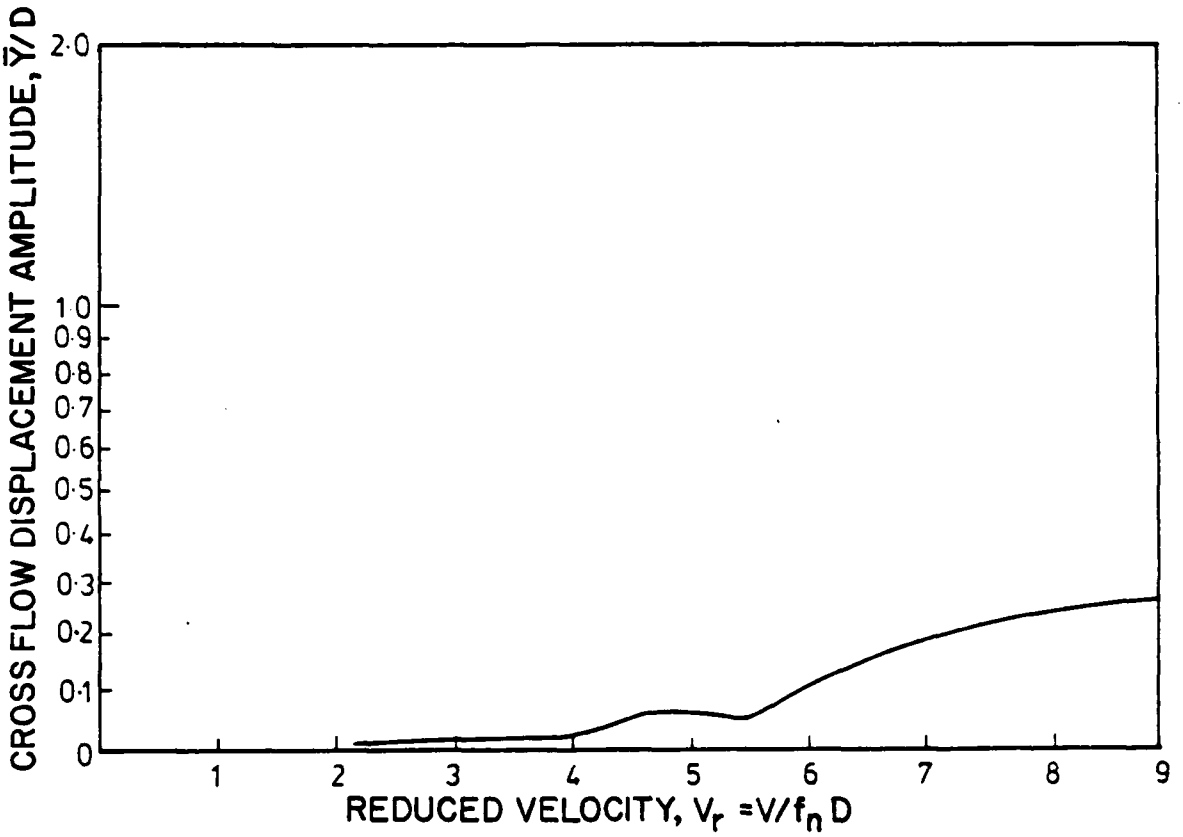

Fig. 15 — The vortex-excited response of the bare cylinder(k_s = 0.44) after it was fitted with a helical strake vortex spoiler (pitch 4.5, protrusion = 10% of the cylinder's diameter) over its entire length; from Every and King [26].

Fig. 16 — Vortex shedding from a drill pipe deployed from the jack-up rig *Ocean Monarch* in the English Channel; from Every and King [27]. A helical strake vortex spoiler is wrapped around the pipe. Prior to the installation of the spoiler, two pipe failures had been caused by vortex-excited oscillations.

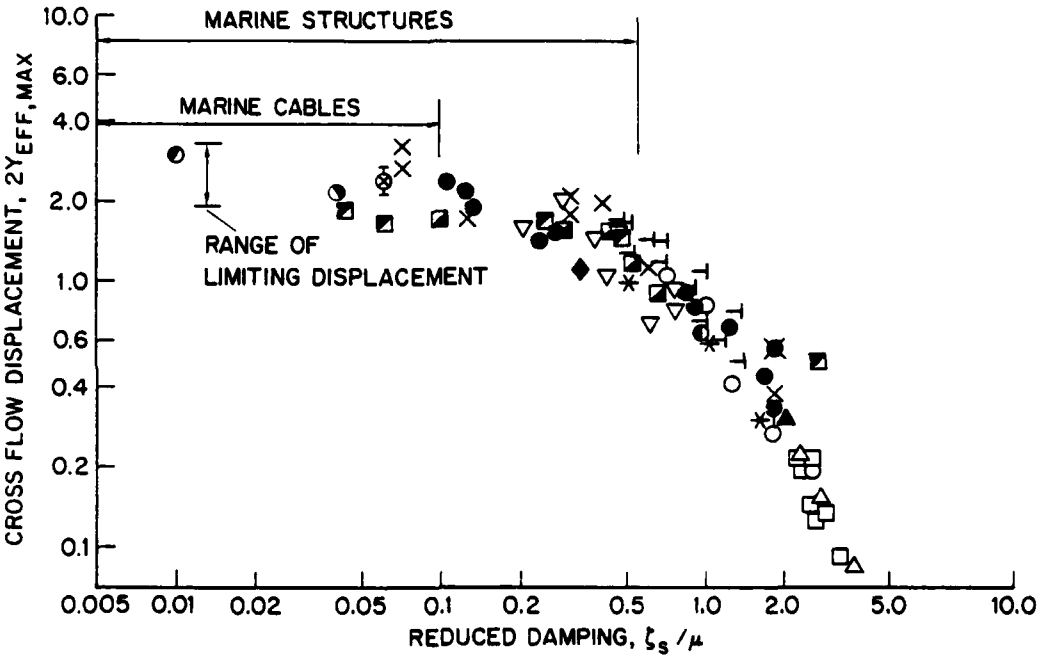

Fig. 17 — Maximum vortex-excited cross flow displacement amplitude $2Y_{EFF,MAX}$ of circular cylinders, scaled as in Eq. (A4), plotted against the reduced damping $\zeta_s/\mu = 2\pi St^2(2m\delta/\rho D^2)$. The legend for the data points is given in Table 4.